Gamma-Gamma Angular Correlations with the GRIFFIN Spectrometer

Lisa Morrison

A dissertation submitted to the Physics Department at the University of Surrey in partial fulfilment of the degree of Master in Physics.

Department of Physics,

Faculty of Engineering and Physical Sciences,

University of Surrey, Guildford, Surrey, GU2 7XH

February 2015

Abstract

The construction of a new γ-ray spectrometer (GRIFFIN) in 2014 allows researchers using the array to investigate more nuclear properties than ever before. The project was successfully completed on schedule, and in September it took its first radioactive beam. GRIFFIN is optimised to house 16 HPGe clovers, each segmented into 4 individual crystals, in addition to auxiliary detection systems, which further increase the detection capability of the array. Alongside the construction of the hardware, an entirely new DAQ system was implemented, allowing faster and more effective data analysis than was possible with the previously-installed 8π array.

The aim of this work was to study the sensitivity of GRIFFIN to angular correlations using a range of γ-ray positioning methods, as well as when 4 germanium detectors are removed to include DESCANT. The consecutive γ-rays arising from the decay of ^{60}Co into ^{60}Ni from the $4^+ \rightarrow 2^+ \rightarrow 0^+$ states were studied, and prior to the first experiment being run, a calibration source of ^{60}Co was mounted in the centre of the array in order to collect this experimental data. Geant4 simulations were also performed by replicating the geometry and properties of GRIFFIN to allow a comparison between expected and experimental results to be made.

It was discovered that GRIFFIN is effective at producing angular correlations of γ-rays, as the shape of the fitted distribution is similar to the theoretical polynomial, and the fitted a_2 and a_4 values are close to theoretical ones. Both the simulation and experiment determined the optimum positioning method to be using single crystal positions with the point at which the maximum energy portion of the γ-ray is deposited taken as its absolute position (with addback).

Finally, the experimental angular distribution was analysed with HPGe clovers 1 to 4 removed, thus replicating the inclusion of DESCANT. This time, the experimental correlation coefficients were closer to the simulated values obtained using 16 detectors, but the optimum positioning method appeared to be using single crystals without addback. Examining experimental results, it appeared that the data for clover 13 was missing, which could account for such discrepancies between experiment, simulation and theory. Overall, these results show that GRIFFIN is able to produce angular correlation information effectively, even when DESCANT is coupled to the array.

Acknowledgements

First and foremost, I would like to thank Professor Paddy Regan, Professor Wilton Catford and Professor Paul Stevenson for arranging my placement at TRIUMF, and therefore allowing me to experience what has been the best year of my life. Of course, I would like to extend my thanks to Dr. Adam Garnsworthy, for giving me the opportunity to become part of the GRIFFIN team and for encouraging me to keep on pushing the limits of my understanding of γ-ray spectroscopy. Without the generous support and guidance from the Gamma-Ray Spectroscopy group, this work could not have been accomplished, and I am eternally grateful for the time everyone took to assist and guide me. In particular, I would like to thank Dr. Jenna Smith for her encouragement, enthusiasm and assistance with all aspects of this work, and for inspiring me to continue in research. My gratitude extends to Dr. Peter Bender, who ensured I understood angular correlations and their origins in nuclear physics, alongside how the GRSISort and Geant codes could be used to produce them. I want to also show my appreciation for the help given to me by Dr. David Miller, Dr. Mohamad Moukaddam, Lee Evitts and the GRIFFIN collaboration based at Guelph, all of whom were always available to help me, no matter how trivial my question was.

It goes without saying that I am indebted to the kindness, patience and generosity shown to me by Shaun Georges, with whom I worked alongside very closely nearly every day during my time at TRIUMF. Thank you for all of your help, advice about where to go in Vancouver, and for cheering me up on the days I found more difficult than others.

Thank you to all of the phenomenal research scientists, postdocs, engineers and students at TRIUMF - you all made my first experience in a 'real-life' laboratory unforgettable. Also, a special thanks extends to those who demonstrated how to use unfamiliar equipment to me, in particular Chapman Lim and his team in the Scintillator Shop, alongside John McKinnon and the Beamlines team.

Finally, I would like to thank my father, for providing me with not just financial support during my time in Vancouver, but also for always being just a phone call away, no matter the time of day. I hope that I have done you proud, and if I am half the parent you are when I have children, then I will know I have done a good job too.

List of Abbreviations

BGO Bismuth Germanate

CFI Canadian Foundation for Innovation

DANTE Dipentagonal Array for Nuclear Timing Experiments

DAQ Data AcQuisition

DESCANT DEuterated SCintillator Array for Neutron Tagging

DRAGON Detector of Recoils And Gammas Of Nuclear reactions

DTL Drift-Tube Linac

ENSDF Evaluated Nuclear Structure Data File

FWHM Full Width at Half Maximum

GEANT Geometry And Tracking

GRIFFIN Gamma-Ray Infrastructure for Fundamental Investigations of Nuclei

GRSISort Gamma-Ray Spectroscopy at ISAC

HPGe Hyper-Pure Germanium

HV High-Voltage

ISAC Isotope Separator and Accelerator

ISOL Isotope Separation OnLine

LEBT Low-Energy Beam Transport

LN_2 Liquid Nitrogen

MAESTRO Multichannel Analyzer (MCA) Application Software

MCA Multi-Channel Analyser

PACES Pentagonal Array of Conversion Electron Spectrometers

RIB Radioactive Isotope Beams

SC-linac Super Conducting linear accelerator

SCEPTAR Scintillating Electron-Positron Tagging Array

SFU Simon Fraser University

SiLi Lithium-Doped Silicon

TIGRESS TRIUMF ISAC Gamma-Ray Escape-Suppressed Spectrometer

TRIUMF Tri-University Meson Facility

UBC University of British Columbia

UVic University of Victoria

ZDS Zero-Degree Scintillator

List of Figures

List of Tables

Contents

Chapter 1

Introduction & Background

GRIFFIN (Gamma-Ray Infrastructure for Fundamental Investigations of Nuclei) is a new state-of-the-art decay spectrometer which greatly improves upon the physics capabilities of the 8π spectrometer previously installed at TRIUMF's ISAC-I (Isotope Separator and Accelerator) facility. GRIFFIN allows for the study of a range of radioactive isotopes using its 16 highly sensitive hyper-pure germanium (HPGe) detectors, and coupled with the ability to add-on a range of auxiliary detection systems, additional decay products can be studied, leading to a detailed analysis of nuclei. Throughout 2013-14, the 8π spectrometer was removed from the ISAC-I hall and moved to Simon Fraser University (SFU) , while the construction of GRIFFIN took place along with the development of a new data acquisition (DAQ) system to process the volume of data produced during an experiment. GRIFFIN was completed on schedule and successfully ran its first experiment in September 2014 studying the isotope Cadmium-116, demonstrating the detection ability and advanced functionality of the spectrometer. In the future, auxiliary detection systems such as the neutron detection array DESCANT (DEuterated SCintillator Array for Neutron Tagging) will be integrated, allowing a greater increase in the physics capabilities already demonstrated by GRIFFIN during its first few experimental runs [2].

1.1 TRIUMF

TRIUMF (Tri-University Meson Facility) is Canada's national laboratory for nuclear and particle physics and is located on the southern tip of the University of British Columbia's (UBC) campus in Vancouver, BC. The facility was established in 1968

through the combined efforts of three renowned Canadian universities: Simon Fraser University, the University of Victoria (UVic) and UBC. Since then, the governing consortium has grown to include a total of 19 Canadian member institutions, and still not only maintains but continues to strengthen its ties to each university along with every student and faculty member [12]. The world-class research infrastructure in place at TRIUMF attracts a variety of international researchers and collaborators, which in turn enhances Canada's global contributions to nuclear, particle and accelerator physics [13].

TRIUMF has an extensive science program in addition to its nuclear and particle physics programs which span a range of research interests including nuclear medicine, materials science and molecular science. The ability of TRIUMF to undertake research in such a wide range of areas is due to the immense physics capability of the on-site cyclotron which accelerates H^- ions up to an energy of 520MeV, before stripping the ions of both orbiting electrons resulting in the extraction of a beam consisting purely of protons. The cyclotron in place at TRIUMF is currently the largest in the world with a diameter of 18m, and has held this coveted title since its completion in 1974 [14]. It is unique in the sense that it accelerates H^- ions rather than protons, and in doing so allows a proton extraction efficiency of around 99.9999% to be achieved, as opposed to that achieved by initially accelerating protons, which is around 80-90% [15].

1.2 The Cyclotron and Beam Production

The H^- ions are created in the ion source, which consists of a hot filament running through the centre of an aluminium-walled cage filled with hydrogen gas. The filament heats up to such an extent that electrons are released and bombard the neutral hydrogen atoms surrounding them, forming H^- ions in addition to protons. A potential difference of 300,000V is applied across the cage and the H^- ions are extracted and enter the 35m long main injection beamline [16]. Once within the main injection beamline, the ions are focused and steered towards the cyclotron using a series of electric and magnetic fields all while a high vacuum of around $5\text{x}10^{-8}$ Torr and a temperature of approximately 15K are maintained using both vacuum and cryogenic pumps. The combination of a high vacuum and a low temperature ensures that the H^- ions do not collide with other atoms, diffusing the beam and leading to a reduction in beam

Figure 1.1: *The cyclotron undergoing maintenance during a shutdown period [1]*

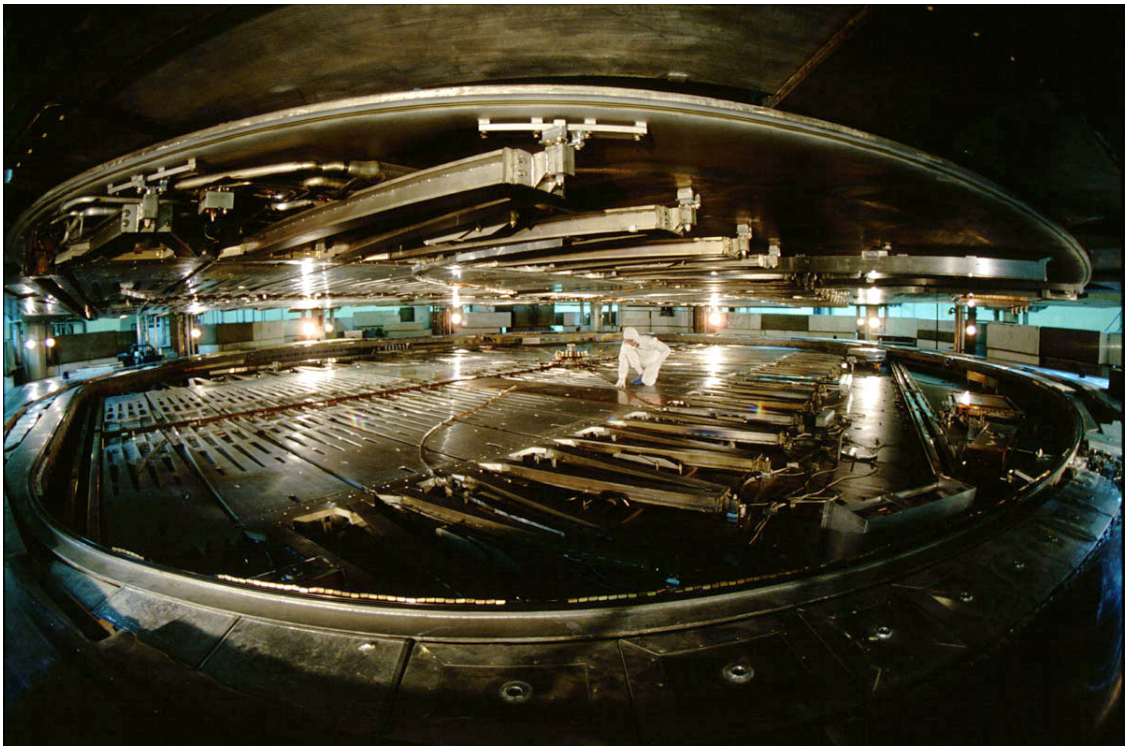

purity as well as potentially causing activation of components within the beamline [17]. The main injection beamline leads the stream of ions directly into the centre of the cyclotron and in-between the north and south pole sectors of the steel magnets, of which there are six of each, totalling 4,000,000kg in weight [18]. As charged particles within a magnetic field experience a force, the action of the cyclotron's magnetic field is to focus the beam of H^- ions into an anti-clockwise trajectory, spiralling outwards as they are accelerated [19]. Acceleration of the ions is achieved using an alternating electric field operating at a frequency of 23MHz produced by electrodes in place within the cyclotron and separated by a small gap. As the ions cross this gap, they experience a 'kick' of energy and the electrodes switch polarity leading to an increase in the radius of the ions' spiral around the cyclotron. This continues until the ions have reached the required energy of 520MeV, which equates to around 75% the speed of light, at which point the accelerated ions strike carefully-positioned thin graphite foils, stripping them of their electrons. The effect of stripping the ions of their orbiting electrons creates a beam consisting purely of protons, and due to their positive charge, the cyclotron's magnetic field causes the beam to be deflected in a clockwise direction and towards one of the four proton beamlines leading to various parts of the TRIUMF site.

1.3 ISAC-I and II Facilities

1.3.1 ISOL Technique

The depth and complexity of physics experiments undertaken at TRIUMF is directly as a result of the ability to create a wide range of radioactive isotopes for use at the experimental facilities. At TRIUMF, the isotopes are created using the beam of protons produced by the cyclotron and the Isotope Separation OnLine technique (ISOL) . The ISOL technique involves aiming the proton beam and striking a carefully-chosen heavy target such as uranium carbide, producing a variety of isotopes through mechanisms such as fission, fragmentation and spallation. In order to separate the required isotope, the cocktail of particles is ionised and then passed through a mass separator, which uses magnetic and electric fields to guide the required ions to the extraction beamline. The ISOL technique results in the production of a high-quality beam with a good energy resolution [20], both of which are fundamental requirements for the experiments undertaken at ISAC-I and II.

1.3.2 Experimental Facilities

Once the required isotope has been selected, it enters the Low-Energy Beam Transport (LEBT) beamline and is accelerated. The LEBT accelerates the beam to around 2% the speed of light, and it is then either sent to the low-energy experimental facilities within ISAC-I, or it enters the Drift-Tube Linac (DTL) and then the Superconducting linear accelerator (SC-linac) , undergoing additional acceleration such that higher-energy experiments can be undertaken in ISAC-II [21]. The capability of producing radioactive isotope beams (RIB) of a range of energies allows the ISAC-I and II facilities to undertake a rich and diverse range of experiments such as: exploring the formation of heavy elements during supernovae using DRAGON (Detector of Recoils And Gammas Of Nuclear reactions) , and to peer into the fundamental nuclear structure of isotopes at GRIFFIN and TIGRESS (TRIUMF ISAC Gamma-Ray Escape-Suppressed Spectrometer).

Chapter 2

GRIFFIN Spectrometer

Decay spectroscopy is a well-established technique used to study the properties and the structure of nuclei, in order to build up the nuclear map of isotopes and advance our understanding of the formation and workings of the universe. In 2011, the Canadian Foundation for Innovation (CFI) , TRIUMF, and the University of Guelph awarded the GRIFFIN project $8.9 million [2]. This investment allowed the collaboration to begin the fabrication and construction of a new spectrometer with enhanced detection capabilities made possible with the use of a set of 16 new HPGe clover detectors. The project was introduced to replace and improve upon the capabilities of the 8π spectrometer, installed at the TRIUMF ISAC-I facility since 2000 [22]. Along with the fabrication of new hardware to accommodate the HPGe detectors and beamline, an entirely new data acquisition system was developed based on the TIGRESS system of acquiring data, and this vastly improves the volume and efficiency of data processing, storage and analysis. GRIFFIN allows physicists to probe weaker decay branches, and determine properties of nuclei which were inaccessible using the 8π spectrometer.

The GRIFFIN spectrometer is designed to be used for low-energy decay spectroscopy experiments, where the radioactive beam being delivered is stopped at the centre of the array and implanted into a moving tape system taken directly from the one used by the 8π spectrometer. The tape system is kept under vacuum to allow decay products from the delivered isotope to be detected, whilst minimising the presence of potential contaminants in the form of unwanted particles usually present in air. Once the beam has been implanted, a period of time known as the 'decay period' passes, during which the decays are measured and counted. The in-vacuum tape is then cycled

and moved out of the centre of the array, into the tape box behind a lead wall. The decay period is chosen such that sufficient decays of interest can occur, and when the tape is cycled out of the array and into the tape box, longer-lived daughter decays and any potential contaminants are removed. This method of decay spectroscopy optimises the signal-to-noise ratio received and processed by the DAQ system, streamlining data analysis procedures and allowing much more data of interest to be acquired [23].

The GRIFFIN array has been designed to accommodate the 16 HPGe detectors in addition to proposed future auxiliary detection systems, and so has a rhombicuboctahedral geometry, with two of the square faces being used as entry for the beam and exit for the tape box. The remaining 16 square faces are designed to house the HPGe detectors, with the triangular faces able to accommodate BaF_2 and $LaBr_3$ auxiliary detectors when required. In addition, the array configuration can be modified to accommodate and couple the DESCANT array, allowing an even greater range of physics phenomena to be studied.

2.1 Detectors

2.1.1 HPGe Detectors

Gamma-ray spectroscopy involves the analysis of complex γ-ray spectra produced during the decay of radioactive isotopes. The range of peaks present within such a spectrum can provide a wide range of information about the structure, lifetime, and decay path of the isotope. However, due to the complex nature of radioactive decay and the presence of contaminant and daughter decays within the sample, a large number of peaks are often visible, and so it is important that individual peaks can be easily resolved. Germanium crystals are ideal for use in γ-ray spectroscopy as they intrinsically provide good energy resolution of γ-rays [10]. Germanium is a semiconductor material and is present between two electrical contacts across which a high voltage electrical field (HV) is applied. This bias voltage (between 3500 and 4000 eV) has to be applied incrementally so as to avoid damaging the crystals and is present in a region known as the 'depletion region'. When a γ-ray enters the detector material and interacts by depositing a portion of its energy, electrons within the germanium are released, and due to the potential difference between the electrodes, these freed electrons move across the

depletion region to the other contact.The charge collected on the electrodes is proportional to the energy originally deposited by the detected γ-ray, and hence the energy of the γ-ray can be determined and displayed on an energy spectrum. The detection capability of the crystals is further enhanced upon purification of the germanium, because the presence of impurities within the crystal causes charge carriers to become trapped. The trapped charge carriers are not detected by the electrodes, reducing the performance of the detectors as a result [24].

Each of the 16 HPGe clovers built for GRIFFIN contains 4 separate 90mm long crystals of germanium arranged in a four-leaf clover geometry. The segmentation of the individual crystals as seen in the TIGRESS array is not required for use in the GRIFFIN array, as the radioactive beam is stopped by the tape and therefore Doppler-shift corrections of γ-ray energies are not required. This means that there are in total 64 individual germanium crystals when all 16 GRIFFIN clovers are mounted in the array. In order to achieve the required close-packed clover geometry, over the first 30mm of each crystal's length, the edges are tapered at 22.5° so neighbouring clovers can be more easily aligned together. When fully aligned, the front face of each HPGe detector is located at a distance of 110mm from the centre point of the array (other distances are possible depending on the experiment), allowing not only the 8π inner vacuum chamber to be accommodated, but also the option of an additional spherical layer of Delrin up to a thickness of 20mm, which works to absorb energetic β-particles which would otherwise be detected as noise in the germanium crystals. In the future, a set of Bismuth Germanate (BGO) shields will be added to the HPGe clovers in order to suppress Compton scattering events occurring within the germanium crystals and as a result improve the position location ability of the detectors [25].

HPGe Efficiencies

Upon the successful completion of acceptance tests undertaken at SFU and their subsequent arrival at TRIUMF, the efficiency and energy resolution of each crystal was tested to ensure it met the required standards set out by the manufacturer and the GRIFFIN collaboration. These properties were tested both using an external Multi-Channel Analyser (MCA) and the DAQ system, primarily to ensure the DAQ system was functioning correctly and reproduced the results demonstrated by the MCA. In order to undertake the required tests on a particular detector using an MCA, each

clover was mounted in a carriage and stand such that it was pointing towards the ground to allow a calibration source (such as ^{60}Co) to be placed within close proximity to the crystals. HV, signal, and bias shutdown cables were attached to both the detector and the MCA, before a bias voltage was gradually applied to each crystal; the voltage applied was either 3500V or 4000V depending on each crystal's stated operating voltage. Using an oscilloscope, the signals generated by the four crystals (each of which is allocated a colour for reference: 'blue', 'green', 'red' or 'white'), were inspected to ensure the crystals were detecting incoming photons as expected and that they weren't damaged. Finally, a calibration source was placed close to the face of the clover and using MAESTRO software [26], a γ-ray spectrum was collected for each crystal within a period of time appropriate to the strength of the source, such that enough counts were collected to sufficiently reduce statistical error. In order to determine the energy resolution of each crystal, the full width at half maximum (FWHM) value of each photopeak was used. The efficiency of each crystal was calculated using the following equation:

$$\text{efficiency} = \frac{N_{actual}}{N_{theoretical}}. \tag{2.1}$$

Here, N_{actual} refers to the net number of counts in the photopeak and $N_{theoretical}$ (the expected number of counts), is calculated using the following formula:

$$N_{theoretical} = A_{source} \times t_{live} \times R_{peak}. \tag{2.2}$$

A_{source} in equation 2.2 refers to the activity of the source used, t_{live} is the live time and R_{peak} is the branching ratio of the transition forming the photopeak being studied. The 1332 keV transition of ^{60}Co was used for both energy resolution and efficiency calculations as this is a well-understood and strong transition. The ideal energy resolution range for each crystal is around 1.9 to 2.5 keV [10], and all of the crystals tested fell within this range using both the MCA and the DAQ system. The efficiencies of the crystals were expected to be very good as a result of the purity of the germanium and the fact that the detectors themselves were very new. Table 2.1 displays the efficiencies of the white crystals calculated for a number of clovers using the MCA. The digitally-acquired values were comparable to analogue results (if slightly higher), both confirming the reliability of the DAQ system and the functionality of the detectors, as their efficiencies were within the expected range. The confirmation of the expected energy resolution and efficiency values will mean that when mounted and closely packed,

Detector	Area$_{net}$	δ(Area$_{net}$)	t_{live} (s)	$N_{theoretical}$	Efficiency	δ(Efficiency)
1	18868	144	7200.00	12675885.212	0.149%	0.001%
6	9731	101	3550.64	6251042.371	0.156%	0.002%
7	9775	101	3331.62	5865448.985	0.167%	0.002%
8	10145	103	3568.32	6282168.711	0.161%	0.002%
9	9964	106	3844.64	6768641.017	0.147%	0.002%
2	9600	101	3519.84	6196817.751	0.155%	0.002%

Table 2.1: *Table displaying the analogue efficiencies of white crystals*

the HPGe clovers will provide a detection efficiency for γ-γ coincidences around 300 times that achieved by the 8π spectrometer.

2.1.2 Auxiliary Detection Systems

The ability to couple a range of auxiliary detection systems to the GRIFFIN array greatly extends the range of physics experiments which can be undertaken using the spectrometer. In addition to γ-rays, a number of other decay products can be detected, and these additional decay products can be used to probe even further into the nuclear properties of the isotope being studied. Three detection systems can be included within the vacuum chamber at the centre of the array; for example, SCEPTAR (Scintillating Electron-Positron Tagging Array) can detect β-particles and find their trajectory, a feature useful in determining which events are as a result of background and which originate from the isotope under investigation. By removing one hemisphere of SCEPTAR, two additional detectors can be added: ZDS (the Zero-Degree Scintillator) which is used to detect β-particles in fast-timing experiments, and PACES (Pentagonal Array of Conversion Electron Spectrometers) which detects electrons produced by the mechanism of internal conversion. In addition, PACES can be used to detect α-particles in experiments investigating heavier isotopes, as the array consists of 5 multi-functional lithium-doped silicon (SiLi) detectors cooled using liquid nitrogen (LN_2) .

Outside of the central vacuum chamber, three additional detection systems can be included. The geometry of the GRIFFIN array is such that it has 8 triangular spaces which can accommodate fast-timing γ-ray detectors used to determine short-lived half-lives of isotopes. Two types of detectors can be used for this purpose: either

any 8 BaF_2 detectors from DANTE (Dipentagonal Array for Nuclear Timing Experiments) or 8 $LaBr_3$(Ce) detectors can be included. In addition, the aforementioned triangular faces of the GRIFFIN array can also house DESCANT detectors if required for a particular experiment - as was the case for an experiment undertaken during December 2014. However, the intended DESCANT-GRIFFIN configuration is such that the 4 downstream HPGe clovers of the GRIFFIN array are removed to make space for the inclusion of the entire DESCANT array. When fully integrated, the coupling of GRIFFIN and DESCANT will allow β-delayed neutron-γ coincidence measurements using low-energy radioactive ion beams to be conducted. Figure 2.2 demonstrates the TIGRESS array configuration with the inclusion of DESCANT, and this is very similar to how the GRIFFIN array will be modified for this purpose [10].

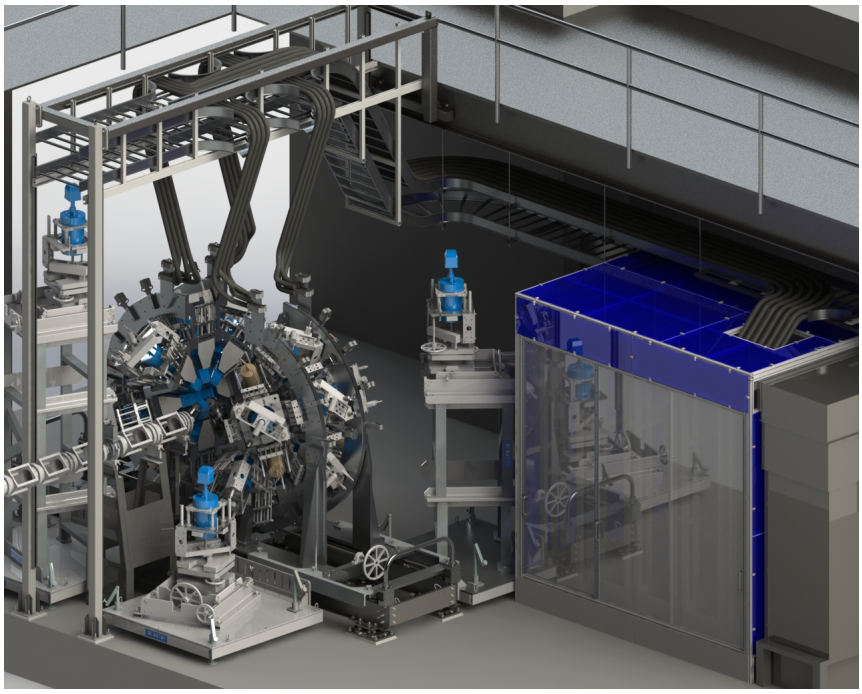

Figure 2.1: *A SolidWorks rendering of the GRIFFIN array, including the electronics shack housing the new DAQ system [2]*

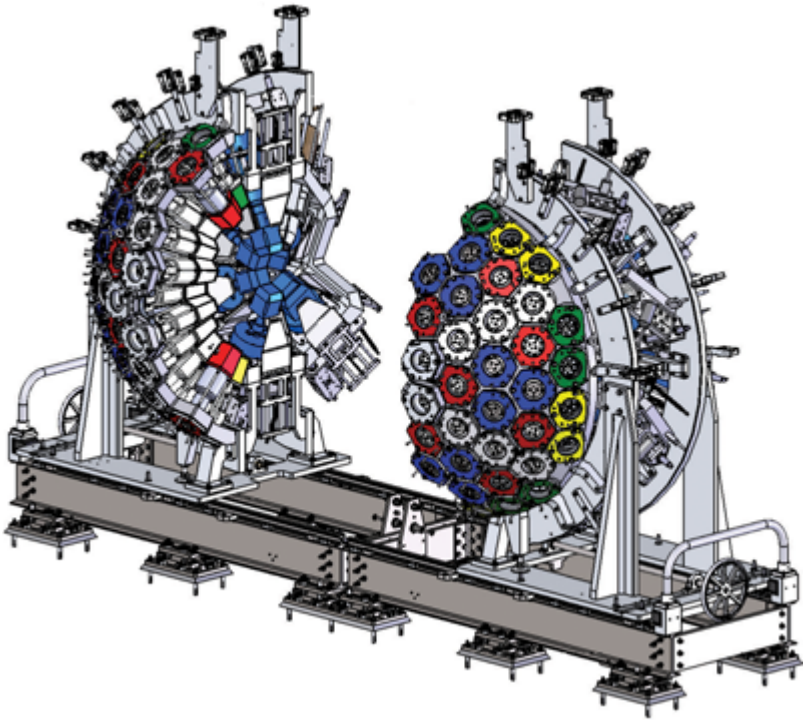

Figure 2.2: *A SolidWorks rendering of the TIGRESS array with the inclusion of DESCANT in place of the downstream HPGe detectors [3]*

Chapter 3

Theory

3.1 Overview

Measuring the properties of γ-rays emitted from radioactive decays can provide a detailed insight into a range of nuclear properties, such as the energies of excited states, as well as their lifetime, spin (J) and parity (π). The reason γ-rays are such a powerful probe of radioactive nuclei is that their energies correspond almost exactly to the spacing between the energy levels from which they originated. γ-rays are highly energetic photons, and can be emitted as a result of the de-excitation of an excited state within a nucleus or as a result of other decay mechanisms such as α or β-decay. By studying the peaks present within a γ-ray spectrum, one can determine the isotope present within a sample (if some information is already known about its level structure) and therefore γ-ray spectroscopy is also a useful technique not only in terms of developing fundamental physics knowledge about an isotope, but also for probing the structure and composition of materials.

3.2 Radioactive Decay

Radioactive decay refers to the process during which a radioactive nucleus goes from an energetic state ('excited' state) to a less energetic state resulting in the emission of a number of decay products. This de-excitation process occurs throughout nature due to the presence of radioactive materials in the surrounding environment, but radioactivity can also be produced artificially (as is done at the TRIUMF-ISAC facility) in order to study the properties of these radioactive isotopes. The process of

using nuclear reactions to produce radioactive isotopes was first performed by Irene Curie and Pierre Joliot in 1934, and since then the technique has developed into a sophisticated method of probing nuclei and their formation [27].

There are three primary processes of radioactive decay which can occur throughout nature (amongst other less common mechanisms): α, β, and γ-decay. Each mechanism can lead to further decays of either type depending on the decay path probability. Each mode of decay produces different decay products characteristic of the decay path taken, and each one of these products provides an insight into the isotope from which they originated. When a nucleus undergoes α or β-decay, an α or β particle is emitted, changing the nuclear species and bringing the radioactive isotope to a more stable configuration, as is favoured in nature. However, a nucleus undergoing γ-decay remains the same nuclear species because no particles are emitted - the nucleus simply decays to a lower, more stable energy state, emitting this excess energy in the form of a γ-ray photon.

3.2.1 Alpha Decay

Alpha decay occurs primarily in heavy nuclei when an unstable nucleus undergoes fission, resulting in the emission of a Helium nucleus (^{4}He), known in this case as an α-particle [27]. The resultant α-particle has a very stable nuclear configuration but is very weakly penetrating, and as a result, α-particles can be stopped by a sheet of paper placed in their pathway. α-particles do however carry a charge of +2 and are therefore highly ionising forms of radiation as compared to other decay products. Equation 3.1 shows an example α-decay which can take place:

$$ {}^{A}_{Z}X_N \rightarrow {}^{A-4}_{Z-2}X_{N-2} + \alpha. \tag{3.1} $$

Although α-particle spectroscopy isn't the primary focus for the GRIFFIN spectrometer, the ability to detect α-particles is made possible with the inclusion of the PACES array, which is useful in experiments involving heavy ion radioactive beams.

3.2.2 Beta Decay

Beta decay occurs throughout nature in a wide variety of nuclei, and as with α-decay, the β-decay process results in the emission of a β-particle, bringing an unstable

nucleus to a more favourable stable configuration. β-particles are electrons or positrons involved in the β-decay process. This mechanism changes the species of nucleus undergoing decay, whilst keeping the mass number (A) the same. Equations 3.2, 3.3 and 3.4 display three types of β-decay which can occur:

$$n \rightarrow p + e^{-} + \bar{\nu}_e \tag{3.2}$$

$$p \rightarrow n + e^{+} + \nu_e \tag{3.3}$$

$$p + e^{-} \rightarrow n + \nu_e. \tag{3.4}$$

Equation 3.2 is called β^{-} decay, Equation 3.3 is named $\beta+$ decay and Equation 3.4 is called electron capture with $\bar{\nu}_e$ and ν_e being an electron anti-neutrino and electron neutrino respectively. The neutrinos cannot be detected by the GRIFFIN spectrometer, however due to the additional auxiliary detection systems, the β-particles can be detected and as such β-decay schemes and β-delayed neutron-γ coincidences (with the inclusion of DESCANT) can be investigated [27].

3.2.3 Gamma Decay

Gamma decay differs from α and β-decay in the sense that the nucleus undergoing decay does not lose or gain any particles, only energy in the form of γ-ray photons is involved in the process. Equation 3.5 demonstrates the basic γ-decay equation:

$${}^{A}_{Z}X^{*}_{N} \rightarrow {}^{A}_{Z}X_{N} + \gamma. \tag{3.5}$$

Although γ-decay can occur in a wide variety of circumstances, it frequently occurs as a secondary mechanism of decay, once another decay (such as α or β) has taken place. This is due to the process of nuclear decay often leaving the nucleus in an 'excited' state which has some excess energy, but this energy is not enough to release another particle. Instead, in order for the nucleus to reach a more stable configuration, its excess energy is released in the form of a γ-ray photon [27].

3.3 Interaction of Gamma-Radiation with Matter

The interaction of γ-rays with matter is fundamental to their detection, as the γ-ray photons themselves usually pass directly through the material comprising the

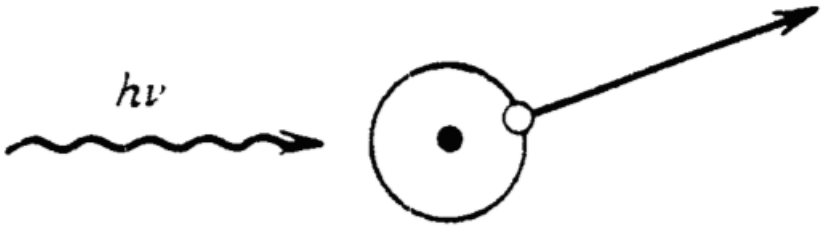

Figure 3.1: *A schematic of the photoelectric effect liberating an electron from its atomic orbital [4]*

detector. In order for γ-radiation to be detected, an interaction within the detector material must occur such that energy is transferred from the γ-ray photon to an electron, which is then detected and its properties traced back to the original incident γ-ray. There are three principal mechanisms through which this γ-e^- interaction can occur: the photoelectric effect (dominant at low energies), pair production (dominant at high energies) and Compton scattering (occurs over a range of energies) [4].

3.3.1 Photoelectric Effect

In γ-ray spectroscopy, the photoelectric effect is the most desired mechanism through which a γ-ray interacts with matter and as a result, detectors are often chosen and optimised to account for this. This effect is dominant at low γ-ray energies of the order of hundreds of keV, and can occur when the incoming γ-ray photon has an energy greater than the binding energy (E_B) binding an electron to its atom within the interaction material. When a γ-ray photon passes through a material, it can be fully absorbed by an electron, and if the energy of the photon $E_\gamma > E_B$ then the electron is ejected from its atomic orbital. The energy of the ejected electron (E_{e^-}) can be calculated with Equation 3.6:

$$E_{e^-} = h\nu - E_B \tag{3.6}$$

where $h\nu$ is the total energy of the incoming photon. When the electrons are detected, their energy can be used to determine that of the γ-ray produced during the original γ-decay of the isotope under investigation. Figure 3.1 displays a schematic of the incoming photon causing the electron to be ejected from its orbital.

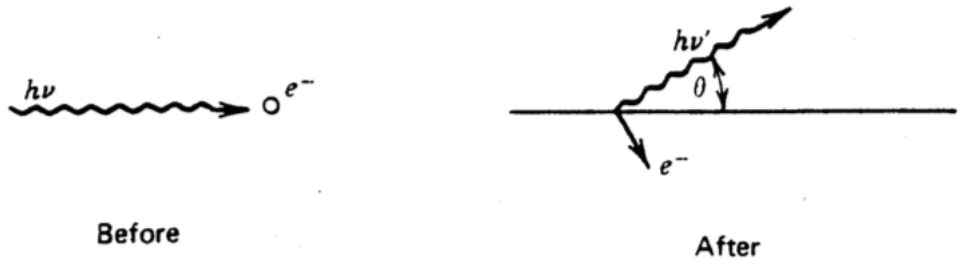

Figure 3.2: *A schematic demonstrating the Compton effect [4]*

3.3.2 Compton Scattering

Compton scattering occurs over a wide range of energies, from hundreds of keV to tens of MeV, and as opposed to the photoelectric effect, which involves a bound atomic electron, the Compton effect involves an interaction between a γ-ray photon and a 'free' or loosely-bound electron. Rather than being absorbed by the electron, the incoming γ-ray photon scatters inelastically, resulting in a portion of the energy of the γ-ray being transferred to the electron which itself recoils. The remaining energy is taken away by the scattered γ-ray which, along with the electron, recoils at an angle dependent on the proportion of the total energy carried away by each. The change in the energy of the γ-ray results in a change of wavelength which is known as the 'Compton shift' and can be calculated using Equation 3.7:

$$\lambda^{'} - \lambda = \frac{h}{m_e c}(1 - \cos\theta) \tag{3.7}$$

where λ and $\lambda^{'}$ are the original and shifted wavelength, h is Planck's constant, m_e is the mass of an electron, and c represents the speed of light. The scattered photon can undergo Compton scattering multiple times until it is absorbed by the surrounding material or passes through undetected, as shown in Figure 3.2.

3.3.3 Pair Production

The final important mechanism through which a γ-ray can interact with matter is pair production. In contrast to the photoelectric effect and Compton scattering, the incident γ-ray photon in this case does not interact directly with a particle, but rather the electric field of a nucleus present within the material. In this case, the act of interacting with the field of a nucleus causes some of the energy of the photon to convert

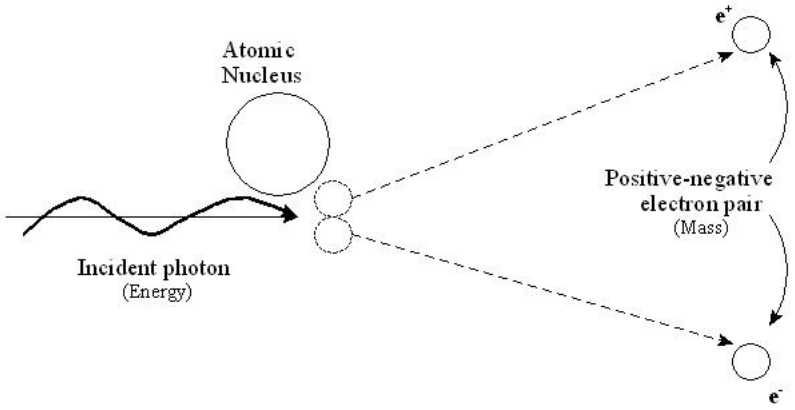

Figure 3.3: *A schematic demonstrating pair production [5]*

into mass, producing an electron and a positron which are a matter and anti-matter pair. As the energy required to create this electron-positron pair is $2m_0c^2 = 1.02$ MeV, where m_0 is the rest mass of an electron, the energy of the incident γ-ray must exceed this value for pair production to occur. If the γ-ray has an energy greater than this minimum value, the electron-positron pair carries away a portion of the excess as kinetic energy, and the remaining energy is carried away by the recoiling nucleus. Although the electron created through pair production is a stable particle, the positron is not, and as such once it has lost a sufficient amount of its kinetic energy, it annihilates with a free electron present in the detector material. Matter and anti-matter annihilation of this type is well-understood and leads to the conversion of mass into energy in the form of two characteristic γ-rays emitted at 180° to one another, each with an energy 0.511 MeV [4].

3.4 Characteristics of Gamma-ray Spectra

All of the aforementioned interactions occur continuously during nuclear decay, and as such a spectrum of counts of γ-rays versus energy (a γ-ray spectrum) is built up over time, allowing a visualisation of the processes taking place. Due to the unique nature in which all of the γ-ray interactions with matter take place, there are a number of characteristic features of γ-ray spectra which can be identified and provide an insight into the properties of the decaying nucleus under investigation. Figure 3.4 displays an uncalibrated example Cobalt-60 γ-ray spectrum with the key features numbered (note

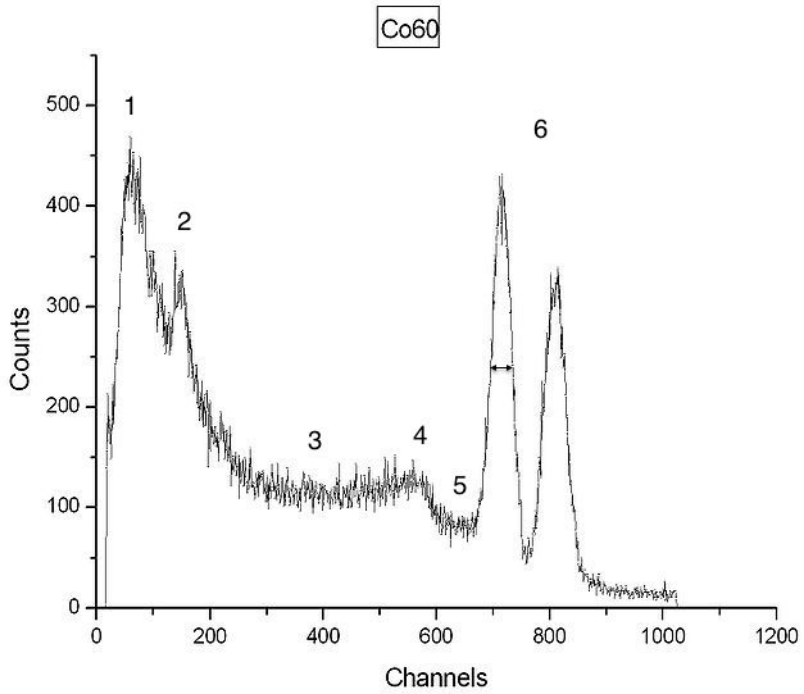

Figure 3.4: *An example Co-60 spectrum [6]*

the inclusion of channel number on the x-axis as opposed to energy):

1. Low energy X-rays: The first and most prominent feature in Figure 3.4 is the peak corresponding to low-energy X-radiation which arises as a result of a process occurring within the atom involving an interaction between its nucleus and an electron in one of its own orbitals. The electromagnetic field of the nucleus interacts with that of the electron, resulting in the electron being ejected from the atom and leaving behind a vacancy which is promptly filled by an electron in a higher-energy orbital. The result of this transition from a higher orbital to a lower one is the emission of an X-ray corresponding to the difference in energy between the levels. This phenomenon occurs frequently throughout nuclear decay, accounting for the large number of counts visible on the γ-ray spectrum.

2. Backscatter peak: This less prominent peak is as a result of γ-ray photons scattering from material surrounding the detectors, some of which re-enter the detector material and their energies measured and included as counts on the spectrum [28].

3. Compton continuum: As previously mentioned, Compton scattering can occur at

a large range of scattering angles between $\theta = 0°$ and $\theta = 180°$, and as a result a large range of energies between the two angular extremes are reached. This results in the broad continuum feature seen on γ-ray spectra, and the shape of the continuum varies from one detector to another.

4. Compton edge: This feature can be explained by an second extreme case of Compton scattering: when an incoming γ-ray scatters off an electron at $\theta = 180°$, transferring the largest amount of energy possible to the electron.

5. Valley: A 'valley' is only visible in this case as a result of the high energy resolution of the detectors as there are very few γ-rays with energies between that of the Compton edge and the photopeak. This lack of counts appears on the spectrum as a prominent dip which rises sharply on either side.

6. Photopeaks: These peaks in Figure 3.4 each correspond to the separation in energy between two nuclear levels within the ^{60}Co isotope and arise as a result of complete photoelectric absorption of the incident γ-ray photon. The width of the peaks (FWHM) is determined by the intrinsic resolution of detector used, whereas the number of counts within each peak (the peak area) is determined by the detector efficiency [29].

Naturally, the final γ-ray spectrum will vary in shape depending on the isotope and detector used. Figure 3.5 displays an example γ-ray spectrum as collected by the GRIFFIN spectrometer.

3.5 Angular Correlations of Gamma-Rays

γ-rays provide fundamental information about nuclei, and one such piece of information which can be determined from the distribution of γ-rays emitted during a particular decay is the spin and parity of the states from which they originated or decayed to, depending on the information already available [30].

3.5.1 Angular Momentum

Each nucleon within a nucleus has a set of 'quantum numbers' which define its unique properties: spin (s), orbital angular momentum (l) and total angular momen-

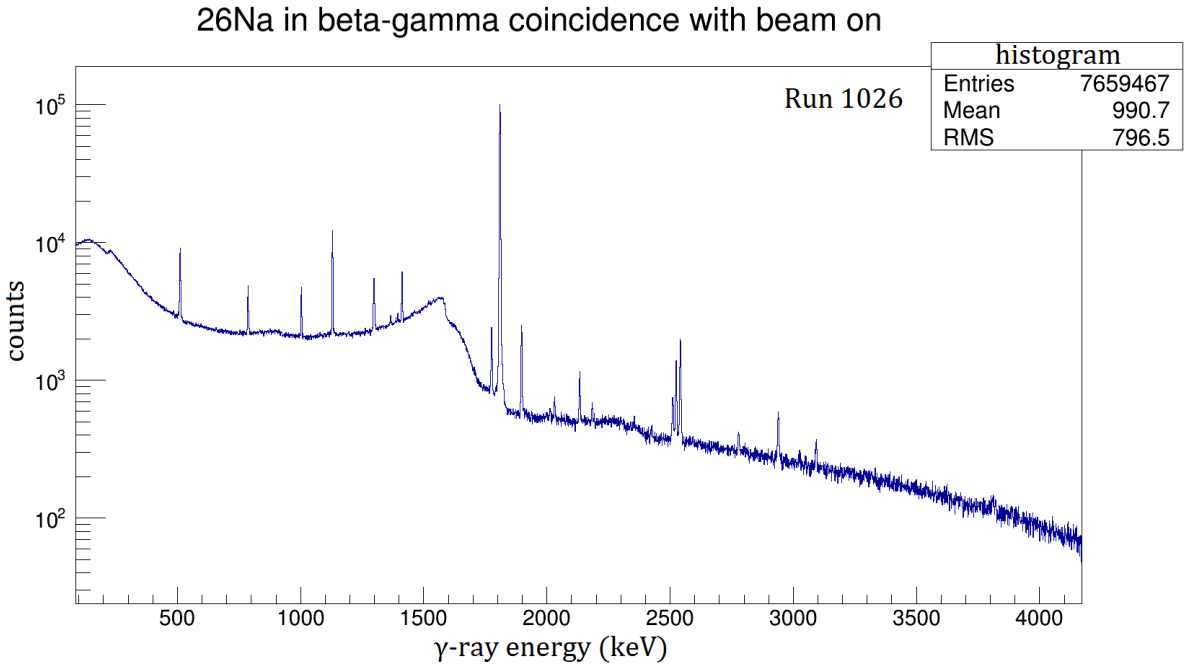

Figure 3.5: *The first γ-ray spectrum collected by GRIFFIN using a radioactive beam [7]*

tum (j), all of which contribute to the overall spin of the nucleus. The total angular momenta $\boldsymbol{j}$ of the individual nucleons sum vectorially to give the total angular momentum of the nucleus ($\boldsymbol{J}$), with a corresponding quantum number J. This quantum number J is used to quantify the total angular momentum (spin) of the particular level in which the nucleus is residing. Therefore, measuring the value of J allows the state in which the nucleus is currently residing to be characterised, and performing this measurement over time leads to the construction of a complex nuclear level scheme. The total angular momentum of a state can have a range of positive or negative integer or half-integer values, depending on the j values of the nucleons [27].

3.5.2 Parity

The second property used to label the state of a particular nucleus, and hence the level in which it resides is the parity (π). This can only take two forms: $+$ or $-$. This property of a nucleus refers to the symmetry of its wave function and whether it appears identical upon reversing its spatial coordinates. As such, $\pi = +$ is known as 'even' parity, whereas $\pi = -$ is known as 'odd' parity. The complete label given to a nucleus and thus its nuclear level is a combination of the total angular momentum and the parity (J^{π}), seen labelled in figure 3.6 [31].

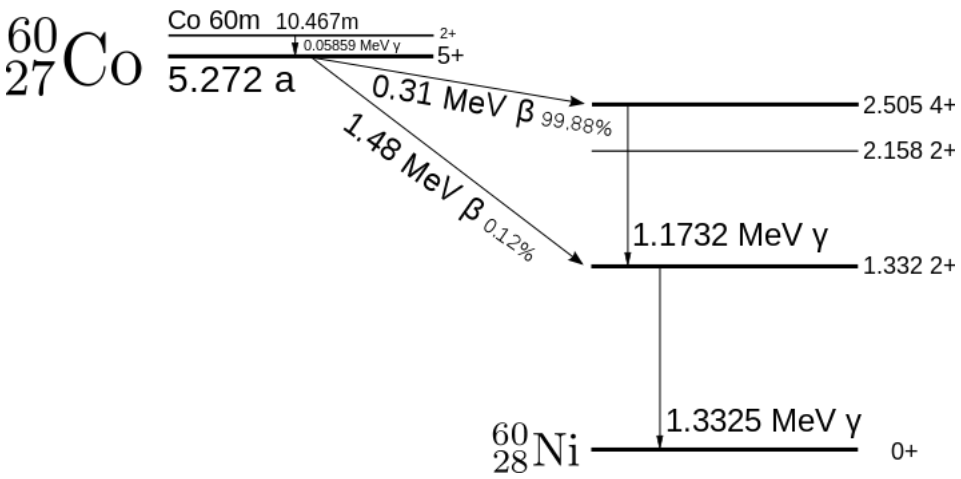

Figure 3.6: *An example Co-60 decay scheme with the spins and parities of the individual levels labelled [8]*

3.5.3 Determining the Multipolarity

Determining the spin and parity of a nuclear state is vital in forming a detailed level scheme for the nucleus, however J and π are difficult to measure experimentally due to the complex nature of the two properties. One way of determining these values is by studying the angular distribution of two γ-rays emitted from the decay of an excited nucleus, as long as the γ-ray photons chosen are known to be consecutive (one decay 'feeds' the other). In sources, due to the random orientation of the nuclei undergoing decay, the first γ-ray of a cascade (γ_1) is not emitted in any particular direction and as such, by gating on the energy of this photon, it would appear to be emitted isotropically. However, once γ_1 has been emitted, the nucleus is left in a certain orientation, and therefore if the direction of emission of the second γ-ray (γ_2) is measured with respect to the first, the true angular distribution of γ-ray photons can be determined [32].

Each γ-ray emitted from a transition between two nuclear levels must follow fundamental conservation laws, and therefore must carry away angular momentum equivalent to the difference between these two levels. This can be expressed using Equation 3.8, where J_i is the spin of the initial state, J_f is the spin of the final state and L is the angular momentum carried away by the photon:

$$\boldsymbol{J}_f = \boldsymbol{J}_i - \boldsymbol{L} \tag{3.8}$$

The emitted γ-ray can therefore be expressed in terms of its multipole order, determined

by: 2^L, for example: if $L = 2$, the emitted radiation is of the order of 4 and is quadrupole radiation. Due to the range of possible angular momentum values ($|J_i - J_f| < L < |J_i + J_f|$), there can be a range of different orders of radiation emitted during one transition, and as such the total radiation emitted can be a mixture of orders of radiation. This mixing can be calculated using the mixing ratio (δ) in Equation 3.9, and provides an insight into nuclear structure [27] [33]:

$$\delta = \frac{< L_2 >}{< L_1 >}. \tag{3.9}$$

The second property of the emitted γ-rays is whether they are of electric or magnetic type, and this is determined by whether or not there is a change in parity between the two nuclear levels and by the multipolarity:

$$\Delta\pi = \text{yes (odd electric, even magnetic)} \tag{3.10}$$

$$\Delta\pi = \text{no (even electric, odd magnetic).} \tag{3.11}$$

Therefore, for the range of possible L values, there are a finite number of multipolarities of the emitted radiation; for example, if $J_i = \frac{5}{2}$ and $J_f = \frac{7}{2}$ and $\Delta\pi =$ yes, the range of possible L values are: $L = 1, 2, 3, 4, 5, 6$. The possible multipolarites of the γ-rays of this type are: $E1, M2, E3, M4, E5, M6$ and as such the radiation emitted during such a transition will be a mixture of all of these possible multipolarities [34].

3.5.4 Angular Correlations

The angular correlations of consecutive γ-rays emitted during a decay are useful in determining their multipolarities, and as a result, the most likely values of the spin and parity of the states from which they originated [35]. With respect to γ_1, the correlation of the emission of γ_2 can be represented by the angular distribution function $W(\theta)$, where θ represents the angle between the direction of emission of γ_2 with respect to γ_1:

$$W(\theta) = 1 + a_2 P_2(\theta) + a_4 P_4(\theta). \tag{3.12}$$

The components a_2 and a_4 are known as the 'angular correlation coefficients' and are calculated using the L and J values of each level and photon involved in the transition, where P_2 and P_4 are Legendre polynomials. It is therefore evident that by experimentally measuring the angular correlations of two consecutive γ-rays, the multipolarities

and mixing ratios of the photons can be calculated, and as a consequence, the J^{π} values of each level can be assigned or (if already known), verified [9]. For a more detailed mathematical derivation of Equation 3.12, please refer to: [36], [37] and [38].

Chapter 4

Simulations and Angular Distribution Algorithms

4.1 Summary

The outcome of a particular experiment can often not be determined by theory alone due to unknown or undetermined variables. In the case of the GRIFFIN spectrometer, it is useful to perform simulations of experiments in order to determine the expected results and whether or not the fabrication, construction and alignment of the hardware have been correctly completed. In addition, although the energy resolution and efficiency of each HPGe detector has been tested individually prior to installation, by comparing simulated and experimental data, one can characterise the performance of the array as a whole in order to establish whether or not it reproduces the physics of a particular decay. Finally, it is difficult to predict how well the spectrometer can reproduce the physics of an interaction when an auxiliary detection system is installed, such as in the case of the removal of 4 HPGe detectors in order to include the DESCANT array, so a simulation is to demonstrate this. Therefore, by simulating a number of decays of a particular isotope, plotting the results, and comparing with experimental data, one can see whether reality agrees with expectation.

4.2 GRIFFIN Simulation Code

Due to the highly random nature of the emission of decay products, the method most appropriate for simulating radioactive decay is by running Monte Carlo simulations. One such piece of software used for many TRIUMF-ISAC simulations and which implements the Monte Carlo method is the GEANT4 (GEometry ANd Tracking) software, itself written and maintained by a collaboration based at CERN and used across the physics community to simulate both nuclear and particle physics events [39]. The software is complex and allows for the inclusion of a range of parameters so as to accurately reproduce the conditions present at the time of a particular physics event. For example, the software is able to model parameters such as the geometry, material and alignment of detectors, as well as providing the ability to track a physics event from parent to daughter decays. Geant4 includes a database of nuclear isotopes, decay paths, and products taken from the ENSDF (Evaluated Nuclear Structure Data File) database and which is frequently updated to ensure the physics remains accurate and all possible interactions can be modelled [40].

Prior to the installation of GRIFFIN, a collaboration based at the University of Guelph wrote a Geant4 code reproducing all aspects of the GRIFFIN spectrometer, from the alignment of the HPGe detectors to the installation of auxiliary detectors such as PACES, SCEPTAR and DESCANT. In addition to being able to visualise a physics event, running the GRIFFIN code results in output in the form of a ROOT file (ROOT is a data analysis tool produced by another collaboration at CERN [41]) containing a range of data which can be analysed and manipulated in order to display the particular physics process under investigation. The data file contains a variety of parameters, such as the number, coordinates, energy deposited and timestamp of an event, allowing a single decay to be tracked from its origin to its daughter decay products and their interaction with the detector material. The GRIFFIN code is therefore a highly flexible tool to determine the optimum capabilities of the array and its results are useful to compare with those collected during an experiment performed by GRIFFIN so as to test the functionality of the simulation, detector and the DAQ system as a whole. Figure 4.1 demonstrates the ability of the simulation to construct the GRIFFIN array based on its geometric parameters.

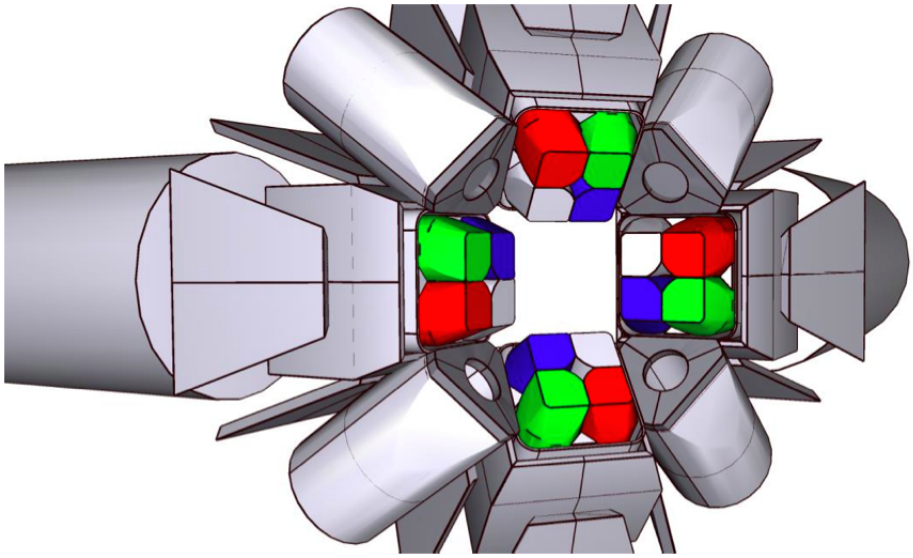

Figure 4.1: *One hemisphere of the GRIFFIN array, as modelled using Geant4 simulations [9]*

4.3 Geant4 Angular Correlations Extension

Alongside the development of a Geant4 code to simulate physics events using GRIFFIN, the collaboration based at Guelph wrote an additional feature which can be merged into the Geant4 software to allow γ-γ angular correlations to be modelled and subsequently visualised. The code contains a condition which changes the emission of radiation from being purely isotropic in nature to being emitted in a certain direction relative to the orientation of the nucleus from which it is emitted. There are no new classes included in this modification, rather the code modifies a number of aspects in the radioactive decay and photon evaporation modules which already exist as part of the Geant4 framework. In addition to this modification, in order for angular correlations to be modelled accurately, a file needs to be input by the user which contains information about the multipolarity of the γ-rays involved in the transition, as well as a second file with information about the ground state angular momentum of the daughter nucleus [9]. Only by modifying these input files can different isotopes and their properties be simulated, and as a result it is important that the information is correctly sourced from the corresponding folders in the Geant4 source files containing ENSDF information. The only information not included in the database is information on the spin and parity of the nuclear levels. This file is created by the user and included within the run macro to be executed during a simulation (see Appendices A and B). The macro

(an executable containing the simulation commands to be run) to be executed during a simulation contains the file path to the tailored input files. So that the conditions of the simulated decay under investigation remain as close to reality as possible, the macro includes all of the decay mechanisms present during an actual radioactive decay, such as the production of auger electrons. These additional physics processes, though not directly relevant to angular correlations of γ-rays, could potentially affect the emission or detection of γ-ray photons, so it is important to take this into account. These additional simulation parameters should allow a clear comparison between the predicted and experimental ability of GRIFFIN to detect the angular distribution of γ-rays.

4.4 γ-γ Correlations Code

The GRIFFIN code requires an input macro corresponding to the chosen isotope in order to reproduce the physics interactions under investigation. Once the simulation code has been run using the chosen isotope (in this case ^{60}Co), the ROOT file can be analysed in detail in order to determine the angular distribution of γ-rays and assign multipolarities to the energy levels. A specially written C++ algorithm was written in order to carry out this analysis using a number of data parameters produced in the ROOT file such as the detector number, coordinates and energy deposited. However, although Geant4 is a powerful and flexible tool for use in modelling radioactive decay, the GRIFFIN HPGe detectors cannot locate the position of the deposition of energy of a γ-ray as precisely or accurately as the simulation can. When a γ-ray enters a particular crystal and is detected, only the centre position of the crystal within which it interacted can be determined. Therefore, the angular correlations algorithm must include a repositioning condition such that the position of a γ-ray is assigned according to the centre of the crystal or detector in which it interacts. The repositioning is made more accurate by using the position coordinates given by experimental data, and as such the simulation becomes much more representative of reality as it takes into account the finite detection capability of the array as determined by the size of each individual crystal. By using the same position coordinates, it also becomes easier to directly compare simulated and experimental results. The finite detection ability arises as a result of the detector material, germanium, which although provides good energy resolution and efficiency values, does not provide very precise position information.

Position information can be improved upon further segmentation of the individual crystals, as is necessary for the TIGRESS array [42].

4.4.1 Addback Modification

The γ-γ correlations code has to contain a modification to account for the necessity of the inclusion of a data analysis technique known as 'addback', something which is automatically accounted for during experimental analysis. The technique is used due to the fact that when a γ-ray Compton scatters within one crystal and into another (or entirely out of the array), only a portion of its total energy is deposited in the first crystal. It is therefore possible for the remaining energy, or a fraction of this energy, to be deposited in a neighbouring crystal. As a result, if this secondary scattering isn't accounted for, fewer counts will be detected in the photopeaks displayed in the spectrum and a greater number of counts will be visible at lower energies, skewing the final results. By summing the energies deposited in neighbouring crystals, the full energy value of the initial γ-ray can be determined once again. A γ-ray can Compton scatter multiple times within the same crystal, and in the experimental data, this scattering is still read out as one charge and therefore one event, as the values are limited by the size of each crystal. However, in the simulated data, the multiple scattering of a single γ-ray is read out as individual events due to the ability of Geant to position the γ-ray to a precision smaller than the size of an individual crystal. The simulation does not therefore treat the Compton scattering in the same way as the experimental data does, and thus the data produced by the simulation must be manipulated so that it treats the interactions in the same way as is done by the 'real' detectors.

4.4.2 Techniques and Algorithms used to Produce Angular Correlations

In order to visualise the effectiveness of the GRIFFIN array at measuring angular correlations, three different C++ algorithms have been written which utilise different algorithms to calculate angular correlations. The first algorithm uses the coordinates of the centre of each crystal in which the full energy γ-ray is detected without accounting for addback, and as such 64 different sets of coordinates are possible. Next, the code was modified so as to take into account only the clover within which the γ-ray is

detected and changes the spatial coordinates of each γ-ray to be at the centre of each clover rather than each crystal, providing 16 different spatial coordinates and greatly reducing the number of data points which can be plotted. The final modification made to the code uses individual crystal positions including an addback modification, and sets the coordinates for each γ-ray based on the position of the portion of the γ-ray which deposits the greatest amount of energy. Appendices C and D contain the algorithms used to produce experimental and simulation angular correlations.

In addition to visualising angular distributions using 16 clovers, the experimental algorithms were modified so as to take into account only 12 HPGe detectors. Detectors 1 to 4 are removed when DESCANT is coupled to the GRIFFIN array, and as such it is important to discover whether the ability of the remaining HPGe detectors to reproduce the expected angular correlations plots is maintained in this case.

Chapter 5

Results and Data Analysis

5.1 Overview

The level scheme of ^{60}Co is well understood and as such is often used throughout the nuclear physics community as a calibration source, in addition to using it to test the functionality of detector hardware systems. Such is the case for the GRIFFIN spectrometer, and prior to its utilisation in experiments using radioactive beams, the ability of the GRIFFIN array to reproduce the angular distribution of γ-rays was investigated using ^{60}Co as the test source. Before the completion of the hardware, a number of simulations were run with the GRIFFIN simulation code using a macro of ^{60}Co which included a range of information on its nuclear properties, such as level schemes and multipolarities. This would allow the visualisation of the angular distribution of γ-rays which could then be compared to the experimental results once the array was run.

The decay under investigation is the decay of ^{60}Co to the ground state of ^{60}Ni which is a $4^+ \rightarrow 2^+ \rightarrow 0^+$ transition resulting in the emission of 2 characteristic γ-rays with energies of 1173 and 1332 keV. As previously discussed, in order to follow conservation laws, each γ-ray must carry away a particular value of angular momentum and parity corresponding to the transition, and for the simulations performed to test the functionality of the GRIFFIN array, each γ-ray was assumed to be of multipole order E2. In reality, there is the possibility during radioactive decay for γ-rays to have a range of multipolarities and as such the transition becomes a 'mixed' transition, however for the simulations run in this case, the γ-rays were set to be unmixed. All of the known energy levels were included in the simulation macros in order to make

the simulation as realistic as possible, and due to the Geant4 data files being sourced directly from the ENSDF database, the level schemes for both isotopes will be up to date.

5.2 Normalising for Array Geometry

The close-packed geometry of the GRIFFIN array is very effective at detecting γ-rays over a large solid angle. However, the rhombicuboctahedral geometry results in a bias in terms of the number of γ-ray angular differences which can be detected as some angles will be detected more frequently than others purely due to the positioning of each clover relative to every other. In order to account for this geometric bias and therefore to visualise the 'true' angular distribution, each plot must be normalised according to the number of clovers installed in the array. Table 5.1 displays the HPGe coordinate table which gives information as to the location of each clover during an experiment and also its alignment relative to the centre of the array. The second array configuration used for determining angular correlations accounts for the inclusion of the DESCANT array which requires the removal of clovers 1 to 4 from the forward lampshades. In order to accurately determine the relative frequency with which a particular angular difference is detected, the exact position of each detector as seen during an experiment is used as the coordinates of the incident γ-ray. This was done by using a data set collected from an experimental run using ^{60}Co, and a C++ code was written using in-built functions from the GRSISort (Gamma-Ray Spectroscopy at ISAC) sorting code to directly retrieve the coordinates of each detector. Using a double-loop structure within the code, once the position of a detector had been found and set as a vector, the angle between that coordinate and the coordinates of every other detector within the array was found, and these values plotted on a histogram. The content of each histogram was then output into a text file, along with the value of the centre of each bin to allow each angular distribution plot to be normalised according to each bin in the normalisation histogram.

For the angular distribution plots using 12 HPGe clovers, the normalisation file had to be modified to account for the fact that the likelihood of certain angular differences to be detected is different as compared to when 16 clovers are used. Two additional IF-statements were included in the normalisation codes in order to account

Position ID	θ lab (deg)	ϕ lab (deg)	Position Description
1	45	67.5	Fore Port Lampshade High
2	45	157.5	Fore Starboard Lampshade Top
3	45	247.5	Fore Starboard Lampshade Low
4	45	337.5	Fore Port Lampshade Bottom
5	90	22.5	Port Corona High
6	90	67.5	Port Corona Top
7	90	112.5	Starboard Corona Top
8	90	157.5	Starboard Corona High
9	90	202.5	Starboard Corona Low
10	90	247.5	Starboard Corona Bottom
11	90	292.5	Port Corona Bottom
12	90	337.5	Port Corona Low
13	135	67.5	Aft Port Lampshade High
14	135	157.5	Aft Starboard Lampshade Top
15	135	247.5	Aft Starboard Lampshade Low
16	135	337.5	Aft Port Lamsphade Bottom

Table 5.1: *A table displaying the coordinates of the HPGe clovers in the GRIFFIN array [11]*

for the missing clovers, and once again the bin contents were output into a text file. Figure 5.1 displays the normalisation histograms for 16 and 12 clovers. There appear to be more counts in each bin for 5.1(a) and in addition, more bins contain counts than in 5.1(b). This indicates that not only is a wider range of angular differences detected using the full number of clovers within the array, but also that more consecutive full-energy γ-rays are detected overall, as is to be expected. However, the overall distribution of each histogram appears to be similar and as such it may not greatly affect the final angular distribution histograms.

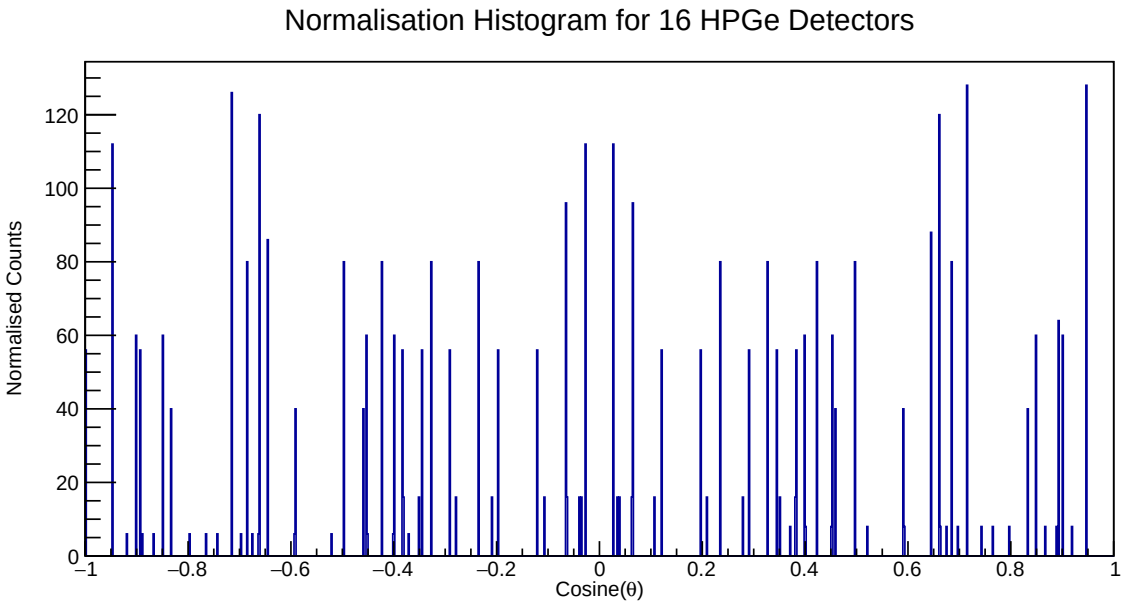

(a) 16 Clovers

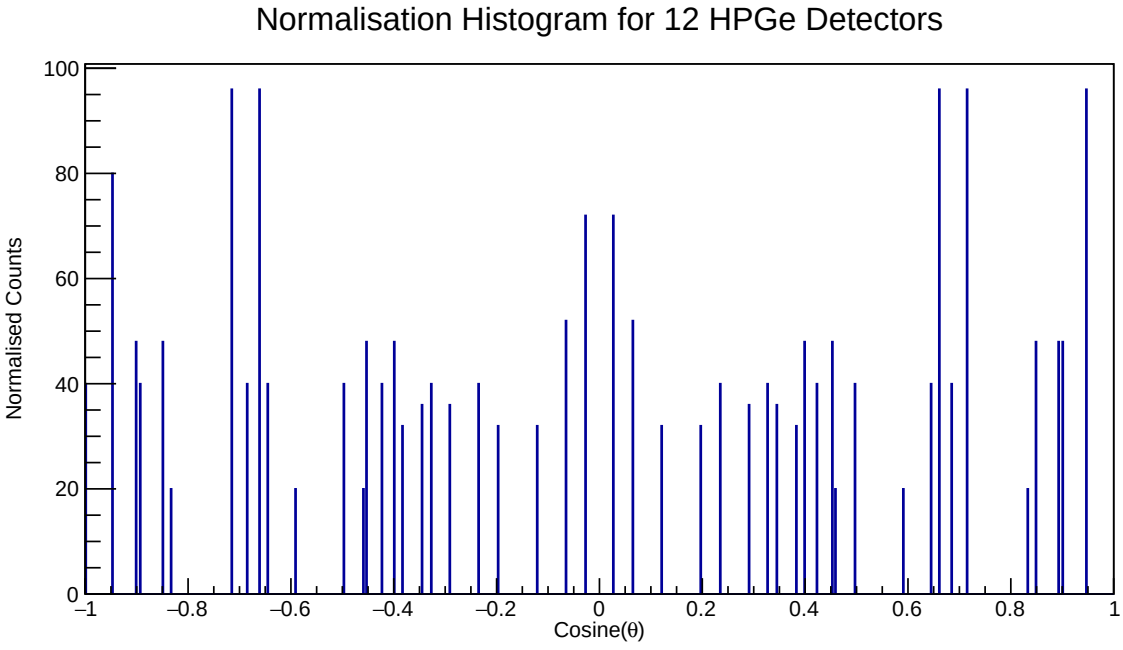

(b) 12 Clovers

Figure 5.1: *Normalisation histograms for 16 and 12 clovers*

5.3 16 Clover Configuration

See Appendices C and D for an example of a code used to produce the simulated and experimental angular distribution plots which follow. Each pair of plots displays the angular distribution of γ-rays determined by using the coordinates of either single crystals without addback, single clovers, or the position at which the full-energy γ-ray deposited the greatest proportion of its energy. In each case the simulation output file and the particular experimental run used for analysis is identical, only the C++ code which analyses the data is altered to produce the three different plot pairs. Each graph displays the results obtained for the cosine of the angular distribution, with the data points fitted using a Legendre polynomial. A separate C++ program was written which utilised in-built ROOT functions to accurately fit a Legendre polynomial to the data points (see Appendix E). The theoretical trend (shown in blue) using the theoretically determined a_2 and a_4 values, is plotted on the same graph in order to allow a visual comparison between the fitted and actual distributions. Figures 5.2, 5.3 and 5.4 display the angular distributions for the simulated and experimental data, differing in terms of the method used to determine the position of the incident γ-rays.

At first glance, there appears to be good agreement between the theoretical and fitted Legendre polynomials in each case, however there are fluctuations in the shape of the curve, depending on the scattering of data points. In addition, the experimental results produced using the calibration source do appear to give similar distributions to the simulation, which suggests that the code, simulation package and γ-γ angular correlations extension are an accurate representation of the physics occurring during radioactive decay. The number of events collected during the experiment was of the same order of magnitude as the number used for the simulation (10,000,000 in the simulation as opposed to 7,681,107 in the experiment). The proportional difference in overall events is reflected in the number of normalised counts produced using the angular correlations code for each pair of plots. This suggests that both C++ angular correlation codes are equally as effective at outputting angular differences between consecutive γ-rays even though they utilise different algorithms and position-mapping methods depending on whether experimental or simulated data is used. Only upon comparing the a_2 and a_4 values from each fitted polynomial will it be evident which method of determining the position of the incident γ-ray is most accurate.

There are no data points at cosine(θ) = 1 because this refers to an angular difference of 0°, which could only occur if the secondary γ-ray is detected in the same crystal as the first. Due to the highly precise nature of the Geant4 simulation, it may have been possible to distinguish these two γ-rays and determine that they interacted within the same crystal. However, due to the time gating used in the DAQ system during an experiment, in reality this interaction would be read out as a single charge which would be the sum of the two γ-ray energies and thus not interpreted separately. As a result, the algorithm used to determine angular distributions for both experiment and simulation was modified such that full-energy interactions within the same crystal were automatically discounted.

A function was written into each angular correlations code which allows error bars for each data point to be displayed in the y-axis. The errors here were calculated using the square root of the number of counts in each bin, normalised according to the corresponding normalisation histogram, for example:

$$\delta \text{ (normalised counts)} = \frac{\sqrt{\text{normalised counts}}}{w} \tag{5.1}$$

where w is the number of counts in the particular histogram bin corresponding to the data point being analysed. The error bars in the x-axis have not been plotted as they are the same for each data point due to the γ-ray position values being extracted directly from the same experimental run for both simulated and experimental data. In addition, the angular distribution fit relies principally on the y-scatter of the data points, not the x-scatter, which is limited to the number of bins set for each histogram. The term 'single detector positions' in the histograms refers to individual clovers in this case.

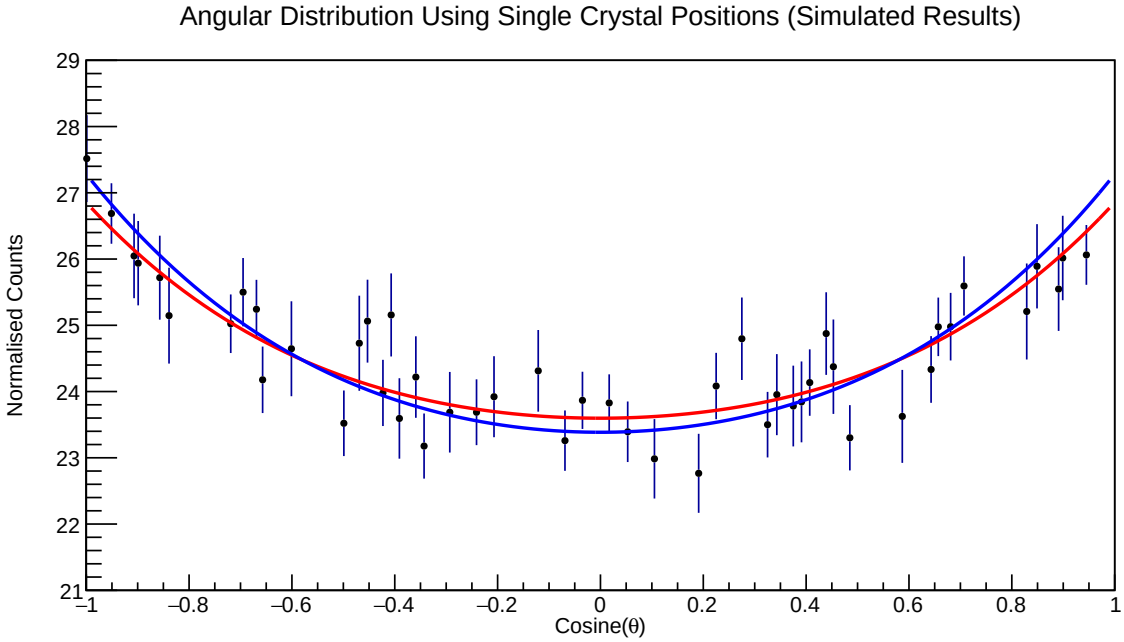

(a) Simulated Result

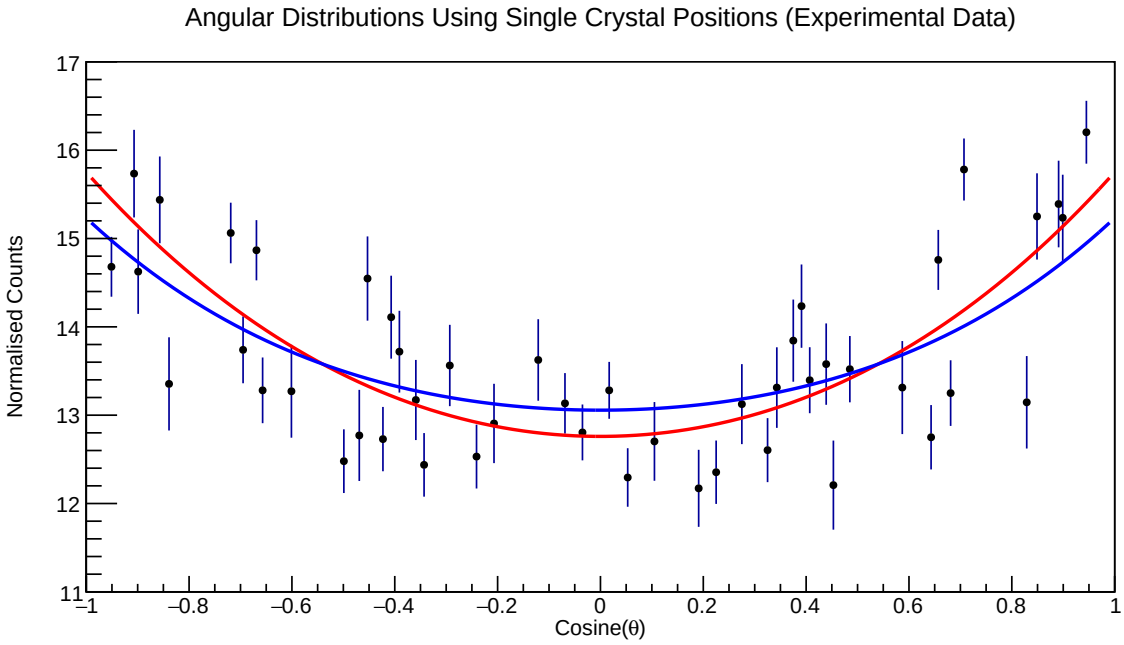

(b) Experimental Result

Figure 5.2: *Graphs displaying the simulated and experimental angular distribution of γ-rays using single crystal positions*

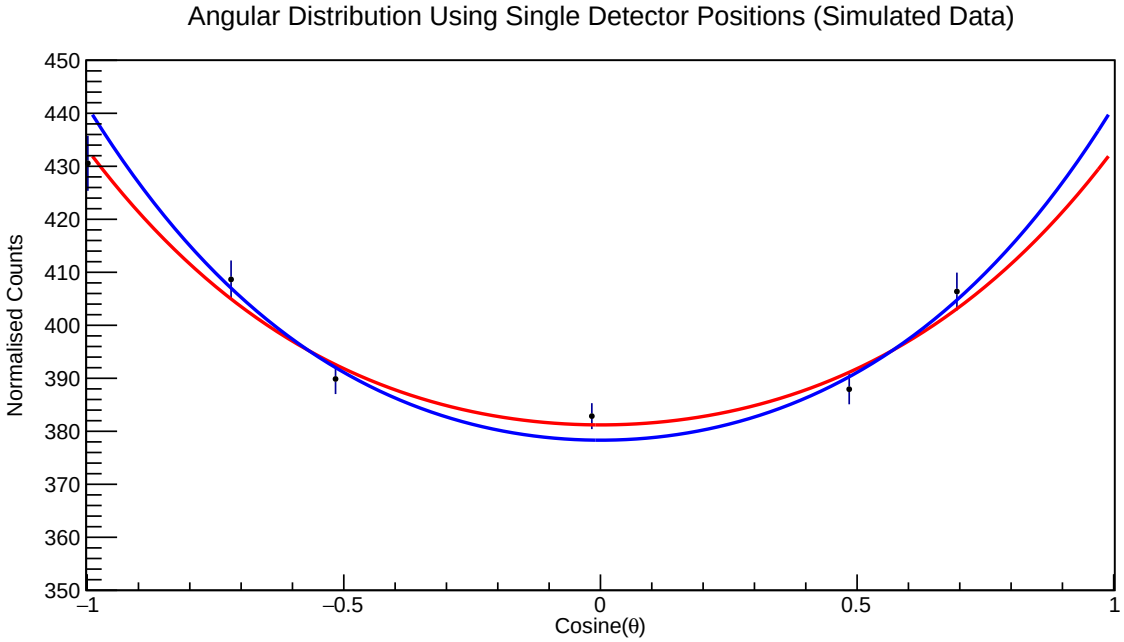

(a) Simulated Result

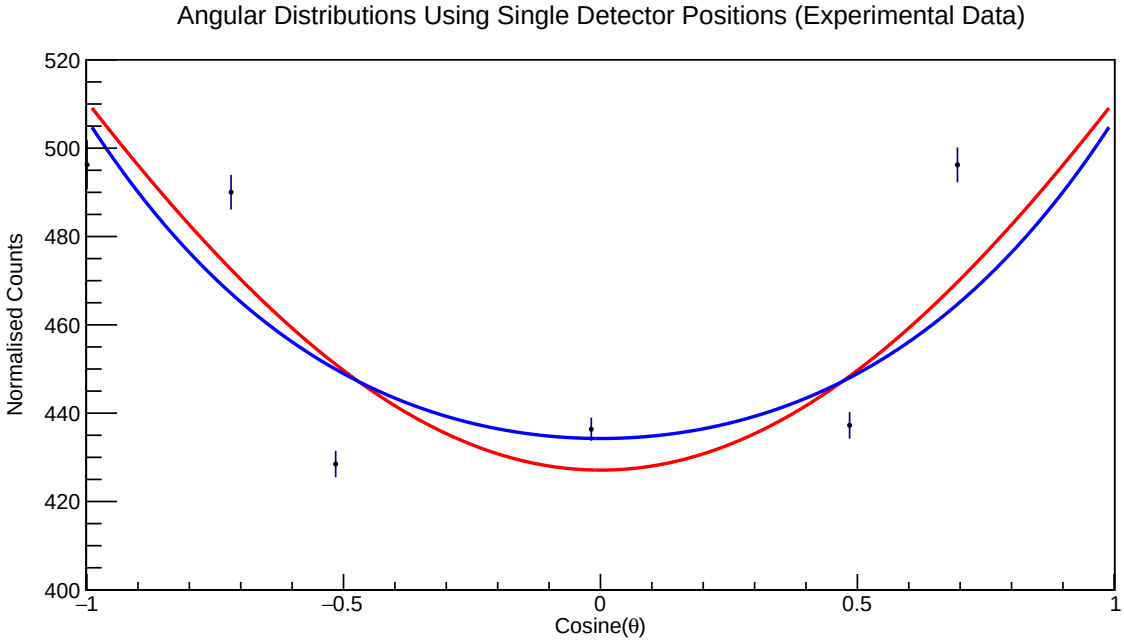

(b) Experimental Result

Figure 5.3: *Graphs displaying the simulated and experimental angular distribution of γ-rays using single detector positions*

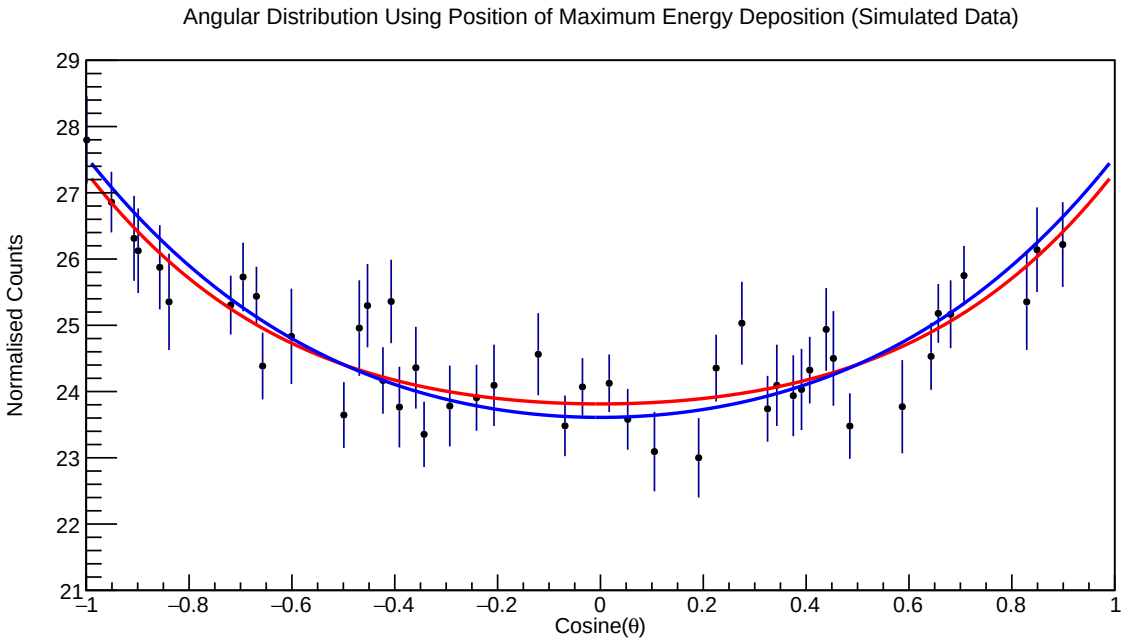

(a) Simulated Result

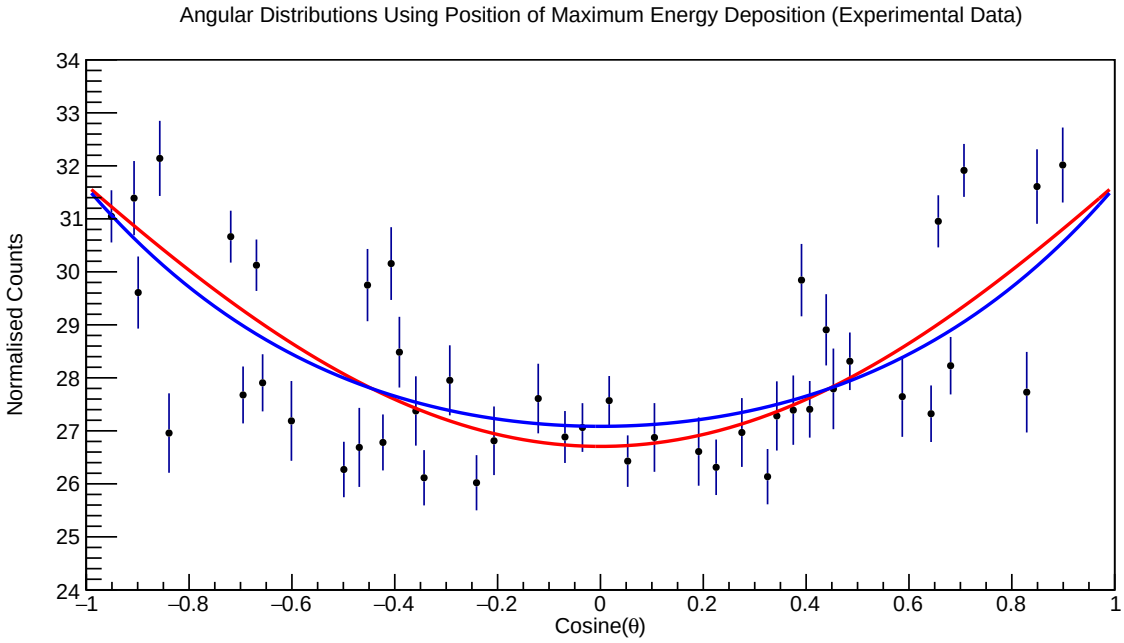

(b) Experimental Result

Figure 5.4: *Graphs displaying the simulated and experimental angular distribution of γ-rays using the position at which the maximum energy portion of the γ-ray was deposited*

	Simulated Results				Experimental Results			
	a_2	Error	a_4	Error	a_2	Error	a_4	Error
Single Crystals	0.085	± 0.007	0.009	± 0.01	0.14	± 0.01	0.004	± 0.014
Single Clovers	0.084	± 0.008	0.007	± 0.008	0.124	± 0.008	-0.005	± 0.007
Maximum Energy	0.088	± 0.008	0.01	± 0.01	0.118	± 0.008	-0.006	± 0.01

Table 5.2: *Table to show Legendre fit values for experimental and simulated data using 16 clovers*

5.3.1 Comparing Simulated and Experimental Correlation Coefficients

The values in Table 5.2 display the fit values produced by ROOT upon fitting a Legendre polynomial to each angular distribution plot. The errors shown in the table for a_2 and a_4 were produced by the ROOT fitting function, not by the Legendre program written to fit the data, and therefore arise purely from the fit of the polynomial to the data points. The correlation coefficients calculated according to theory are: $a_2 = 0.1020$ and $a_4 = 0.0091$, assuming that the transition is unmixed and that the emitted γ-rays are of multipole order E2. Examining firstly the difference between experimental and simulated a_2 values, it appears that the correlation coefficients produced by the simulated data are much closer to theoretical values than the experimental constants, although none are within the bounds of the provided uncertainties. This constant has a greater impact on the overall $W(\theta)$ fit than a_4 due to the larger factors within its corresponding P_2 polynomial, and as such it is the best indicator of how well the expected angular distribution histogram is reproduced from the data. From this initial observation, it appears that the simulation consistently produced more accurate results than the experiment, perhaps due to the 'idealistic' nature with which events are simulated which doesn't take into account potential errors in the equipment used. For example, when examining the energy values produced, the simulated energies appear to be very precise and consistent for each full-energy γ-ray, which is a stark contrast to the spread of the photopeak energy as seen on a γ-ray spectrum. Although an energy gate of 5 keV was chosen when analysing whether a γ-ray resulted from one of the transitions under consideration, it may be the case that a wider energy gate is

necessary to include all relevant photons for experimental analysis. This means that more full-energy γ-rays will be counted in the simulation than in the experiment, simply because they always have the same energies which fall within the specified range. In addition, the simulated a_4 constants are all much closer to the expected values than the experimental constants, however the uncertainties for both data sets are very large compared to the actual value, and as such it is unclear whether experiment or simulation produced more accurate results using these constants alone.

One observation which can be made by looking at the a_2 values produced by the simulation is that they are all within the bounds of uncertainty of each other. It is therefore possible that the results differ from theory by a scaling factor which wasn't taken into account in either the simulation package or the angular correlations code. However, the similarity of a_2 and a_4 for each positioning method could be as a result of the nature in which the Geant4 algorithms track a decaying particle upon its interaction within the detector material. The simulation gives very precise and accurate position coordinates for each γ-ray and as such the angular correlations code was altered so that each coordinate was shifted to be at the centre of the clover or crystal within which the interaction occurred. This should have ensured that the simulation reproduced the positioning methods of an experiment, however it may be the case that simply shifting the coordinates for each event isn't enough to replicate the effects taking place during an experimental run.

5.3.2 Comparing γ-Ray Positioning Methods

Subtracting the fitted correlation constants from the expected ones gives an indication as to which method of determining the position of interaction of each γ-ray is the most accurate representation of reality. By doing so, both the experimental and simulated a_2 values produced using the position at which the γ-ray deposited the maximum energy is the closest to the theoretical value. However, the least effective positioning method varies between the simulated and experimental results, with the single clover positions being the least effective when running the simulation and the single crystal positions being the least effective when analysing experimental data. In fact, the least accurate fit value overall is the experimentally determined a_2 value using single crystal positions, and the magnitude of the difference is almost twice as large (+0.038) as the

next worst fit (+0.022), which suggests that this result may be as a consequence of a mistake in the angular correlations code or crystal mapping for this case. The simulated data determined the least accurate method of γ-ray positioning to be the method using the coordinates of the centre of each clover, rather than the individual crystals. This is expected to be a less effective positioning method as far fewer angular differences can be detected this way, leading to a reduction in the number of data points on the graph. Naturally, the overall reduction in data points leads to a less effectively fitted Legendre polynomial. However, it is important to note that the simulated a_2 constants are all very close together, and as such it is difficult to definitively determine which positioning method is the least effective overall. The agreement between simulated and experimental results as to the most effective method of determining the position of the γ-ray (the maximum energy deposited) enhances the reliability of using this method to determine angular correlations in the future, and supports the assumption made that an incident γ-ray photon deposits the majority of its energy upon its first interaction within the detector material.

Analysing the experimental ROOT file allowed a further investigation to determine why the experimental correlation coefficients are not as close to theory as the simulated values. Due to the largest differences between theoretical and experimental values being when individual crystal and clover positions were used, the hits for each clover and crystal were examined more closely. By accessing the data for each of the 16 clovers, it became evident that one of the clovers was not working or was counting incorrectly at the time of the experiment. Figure 5.5 displays a graph showing the number of counts per clover, and there are no counts for clover 13, which is located in the 'aft port lampshade high' position. The result of missing a clover completely would mean that the normalisations are incorrect because not all angular differences would be measured as frequently as expected. As an entire clover is missing and not just a crystal, every positioning method would be affected and could explain why the experimental correlation coefficients are consistently worse than the simulated values.

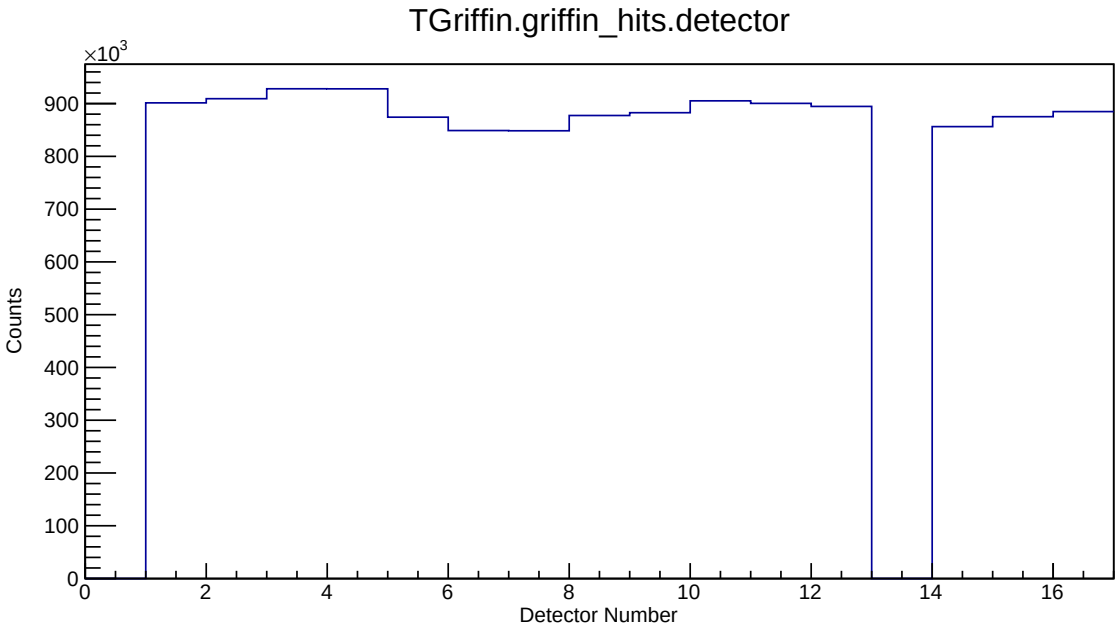

Figure 5.5: *Histogram showing the number of counts per clover for the experimental run used for this analysis*

5.4 Changing the Array Configuration for DESCANT

In early 2015, there are plans to couple DESCANT to GRIFFIN in order to further enhance the physics capability of both arrays. However, in order to do so, 4 HPGe clovers must be removed from the GRIFFIN array in addition to both forward lampshades. Figure 5.6 shows the front of the GRIFFIN array without the forward lampshades, displaying the ring of the corona on which DESCANT will be mounted. DESCANT is an array of neutron detectors, and as a result, by coupling the array to GRIFFIN, the number of γ-rays detected will be reduced. In order to visualise the effect of reducing the number of HPGe clovers by 25% on the ability of the array to reproduce the angular distribution of γ-rays in the decay of ^{60}Co, the experimental angular distribution code was modified. The code utilises the same experimental data along with the normalisation histogram for 12 clovers, but doesn't include the γ-rays incident in clovers 1 to 4. Comparing the correlation coefficients to those obtained using an array of 16 HPGe clovers will provide an indication as to the overall effect of the ability of the array to replicate the angular distributions. Figures 5.7(a) and 5.7(b) display the experimental results using single crystal positions and position of maximum energy deposition of the incident γ-ray. The plot for single clovers had too

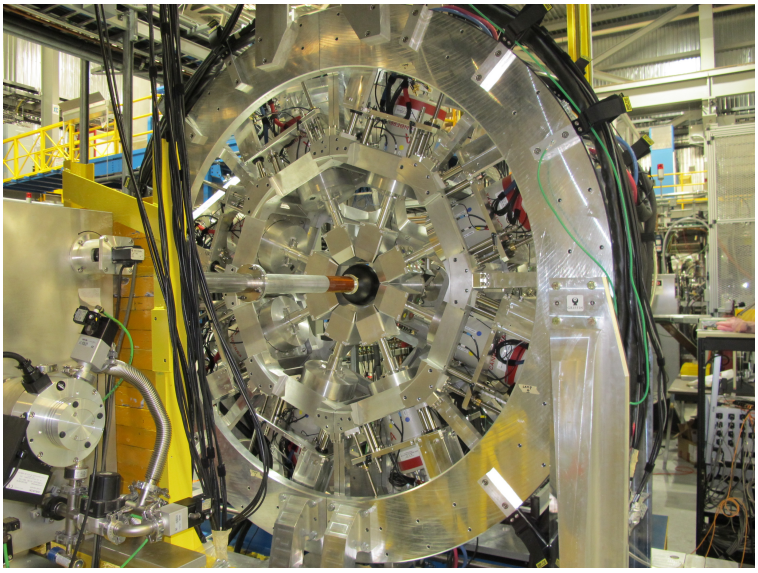

Figure 5.6: *The GRIFFIN array without the forward lampshades in preparation for housing DESCANT [10]*

	Experimental Results			
	a_2	Error	a_4	Error
Single Crystals	0.085	± 0.007	0.009	± 0.01
Maximum Energy	0.07	± 0.01	-0.03	± 0.01

Table 5.3: *Table to show Legendre fit values for experimental data using 12 clovers*

few data points to be able to reasonably fit a Legendre polynomial and therefore isn't included here. The small number of points in the case of using the coordinates of 12 clovers is to be expected due to the fact that there are even fewer numbers of angular differences possible than when individual crystal positions are used, of which there are 48 different coordinates.

Figures 5.7(a) and 5.7(b) display the experimental angular distributions of consecutive γ-rays using 12 HPGe clovers (5 to 16), therefore simulating the addition of DESCANT. It is immediately evident that the asymmetry of these plots is a stark contrast to the highly symmetric nature of the graphs produced using 16 clovers. Only upon analysing the correlation coefficients from fitting these plots will it become clear whether the theoretical angular distribution has been reproduced in this case. Table 5.3 displays the fitted experimental a_2 and a_4 coefficients and interestingly, the experimental results are now much closer to the previously obtained simulated values using

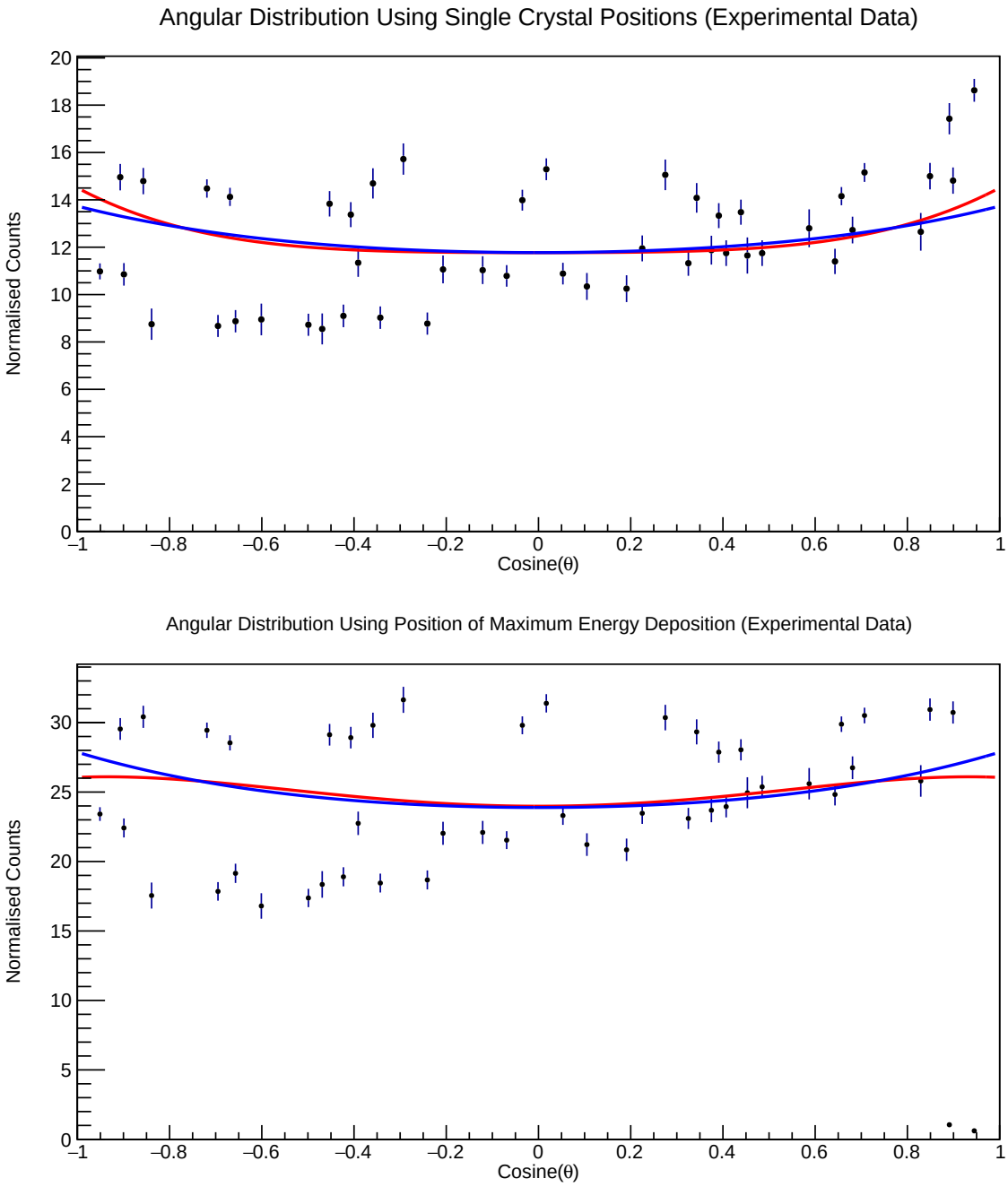

Figure 5.7: *Graphs displaying the simulated and experimental angular distribution of γ-rays using 12 clovers*

16 clovers. In addition, in the previous set of results shown in Table 5.2, the experimental values of the coefficients vary widely depending on the positioning method used. In the case of 12 clovers however, the a_2 coefficients for both positioning methods are both well within the bounds of uncertainty of one other. Finally, it appears that the optimum positioning method in this case is by using the coordinates of the centre of the crystal within which the γ-ray interacted, whereas this appeared to be the least effective method in the case of using 16 clovers. In fact, the a_2 and a_4 values using single crystal positions are much closer to theoretical values than when 16 clovers were used, which suggests that even with the addition of DESCANT to the array, angular distributions can still be reproduced effectively.

The asymmetry in Figures 5.7(a) and 5.7(b) could be as a result of ineffective binning used when plotting the angular distribution histograms prior to normalisation. Both figures display a similar scattering of data points, with fewer counts plotted around negative cosine(θ) values. It could be that simply modifying the angular correlations code so as to discount the first four clovers and using a new normalisation histogram isn't enough to account for potential secondary effects occurring during radioactive decay. For example, the addback function may need to be modified as it could be the case that many γ-ray Compton scattering interactions cannot be 'traced back' to sum to the full-energy values due to a portion of the γ-ray energy being deposited in the discounted clovers.

The change in the optimum positioning method in the case of using 12 clovers may be as a result of an incoming γ-ray depositing its maximum energy in clovers 1 to 4, before further Compton scattering into clovers 5 to 16 and therefore not being detected at all leading to a reduction in the effectiveness of using this method in finding angular differences between γ-rays. The proximity of both a_2 and a_4 coefficients to each other once again suggests that there may be an additional scaling factor which needs to be taken into account in the angular correlations code. One consideration as to why the coefficients differ from theoretical values is the fact that there was a missing clover (clover 13), and therefore instead of 12 clovers, there were only 11 in place during the data collecting period. This wasn't accounted for in the angular correlations code, nor the normalisation histogram, and may contribute to the difference between theoretical and experimental correlation coefficients.

Chapter 6

Conclusions & Further Work

The construction of the new GRIFFIN spectrometer throughout 2014 was achieved through a determined collaborative effort from a number of scientists and engineers. It successfully took a radioactive ion beam and completed its first experiment at the end of 2014 [43], and there are great plans for the spectrometer in the future. The success of the project is evident upon analysis of experimental data. The aim of this work was to determine the ability of GRIFFIN to accurately reproduce the angular distribution of consecutive γ-rays emitted during the decay of ^{60}Co. By comparing simulated angular correlations to results collected during an experiment using a calibration source, it is clear that the hardware, DAQ system and sort code used to analyse GRIFFIN data are effective at reproducing the simulated distributions. A further aim of this analysis was to determine the extent of the effect of removing 4 HPGe detectors on the reproduction of angular distributions and to see which method of γ-ray positioning is the most accurate way to determine the interaction point of the full-energy γ-ray. By determining the optimum analysis methods, it will be easier in future experiments to better extract angular correlations from the data produced during radioactive decay.

By gating on the two full-energy γ-rays emitted during the decay of ^{60}Co from a $4^+ \rightarrow 2^+ \rightarrow 0^+$ state, the simulated and experimental angular distributions upon initial analysis appear to produce similar results. There are more fluctuations in the y range of the experimental data, but this is to be expected as the simulation reproduces a decay under idealised conditions. These simulated conditions do not take into account potential mixing (δ) of the emitted γ-rays, which would change the angle the second γ-ray is emitted relative to the first. Mixing does occur during a 'real' decay, and

as such the experimental results are expected to be further from those theoretically predicted than the simulation. Fitting a Legendre polynomial to both sets of data gives a better indication as to how accurately the angular distribution is reproduced. By examining the correlation coefficients a_2 and a_4 produced during the fitting of each graph, it appears that the simulated results are closer to the theoretical values (the theoretical coefficients are: $a_2 = 0.1020$ and $a_4 = 0.0091$), than those found using experimental data. It is important to note however, that the a_2 and a_4 values were calculated using the assumption that the γ-rays emitted during the decay are unmixed ($\delta = 0$), which is exactly the case used in the simulation. As a result, one would expect the correlation coefficients produced using simulated data to be closer to theoretical values because the 'actual' decay would include some mixing of the multipolarities of the emitted full-energy γ-rays. However, even with the potential mixing of multipoles considered, the experimentally fitted a_2 and a_4 values are still close to theoretical ones, suggesting that the GRIFFIN array is effective at demonstrating angular correlations.

Optimising data analysis procedures is vital during an experiment when lots of data is produced. For this reason, it is important to discover which method of determining the position of interaction of an incident γ-ray (and hence from which to measure angular differences), is most accurate. By doing so, the physics of a decay event can be more easily visualised, allowing conclusions to be drawn from the data more effectively. Three separate methods of determining the position of an incident γ-ray were used in the results above: using the coordinates of single crystals without addback, single clovers with addback, and single crystals using the position at which the maximum energy portion of the γ-ray was deposited. By examining the correlation coefficients, it appears that for both experimental and simulated results, using the position of maximum energy deposition yielded a_2 and a_4 coefficients closest to theoretical values. This supports the assumption made that when a full-energy γ-ray enters the detector material and secondary scattering occurs, the position at which it deposits the largest amount of energy should be taken as the main position for the entire event. In the future, this method of using maximum energy deposition may be more effective than other positioning methods at reproducing angular correlation histograms, however angular correlations using other radioactive isotopes should be studied, as this may not be the case with full-energy γ-rays of higher or lower energy.

A unique feature of GRIFFIN is its capacity to house additional auxiliary detec-

tion systems. One such system is DESCANT, which is planned to be mounted onto the GRIFFIN array in early 2015, in preparation for upcoming experiments. However, installing DESCANT requires the removal of the forward GRIFFIN lampshades which themselves house four HPGe clovers. It is vital that the removal of a quarter of the γ-ray clovers still allows γ-decay physics to be visualised and examined. In order to test the result of removing germanium clovers 1 to 4 on the angular distribution plots produced during an experiment, the code used to determine angular correlations was modified to discount clovers 1 to 4. In addition, a new normalisation histogram was produced to account for the fact that the frequency with which certain angles are detected will vary with a different number of clovers mounted in the array. Examining the plots produced using the single crystal and maximum energy positioning methods, it is apparent that there is some asymmetry in the distribution which wasn't present in the previous plots. This may be as a result of incorrect binning of the histograms, or not having properly accounted for the missing detectors when mapping positions within the angular correlations code. However, upon fitting the Legendre polynomial, the correlation coefficients are closer to theoretical values than those obtained using 16 detectors. The single crystal positioning method yields better results than the maximum energy method, which is a stark contrast to the previous result in which the opposite was the case. From these plots it is difficult to determine which positioning method is best, however they do confirm that when DESCANT is mounted on the GRIFFIN array, angular distributions of γ-rays are still able to be visualised effectively.

6.1 Further Work

In the future, it would be useful to use a number of different radioactive isotopes to determine the angular distribution of consecutive γ-rays, such as Europium-152 which contains a number of these characteristic transitions. In terms of the simulations run for this particular data analysis, there were a number of difficulties which arose as a result of merging the angular correlations extension into the main framework of the GRIFFIN Geant4 code. In order for the simulation to produce effective results, the variable 'G4_Galactic' had to be set so that instead of the isotope being present within a vacuum, as is the case during an experiment, the environment was set to air. In addition, the simulation appeared to be 'dropping' events and as such these were not

included in the final angular correlations plots. Since undertaking this project, these issues have been resolved by the newly updated version of Geant4, and so it would be interesting to re-run the simulations and see whether the fit improves. Continuing to improve the codes used to produce angular correlations such as changing the energy gate or the time coincidence window would also be valuable in determining whether useful events were not being included during this analysis in experimental data.

Finally, investigating the angular distributions using an array with 6 or 8 clovers would also be useful in terms of determining the impact on the results when other auxiliary detection systems are mounted, or when maintenance must be performed on the detectors. It should be the case that angular correlation histograms will become less reliable upon the removal of detectors, although this didn't seem to be the case when 12 clovers were used. However, due to the missing clover in the experimental data which wasn't accounted for during analysis, further research must be done into the impact of removing clovers on angular distributions before any clear conclusions can be drawn.

Appendix A

^{60}Co Simulation Macro

```
#/DetSys/world/material G4_Galactic

/DetSys/det/SetCustomShieldsPresent 0
/DetSys/det/SetCustomRadialDistance 11 cm
/DetSys/det/SetCustomExtensionSuppressorLocation 1
/DetSys/det/includeGriffinHevimet 0

/DetSys/det/SetCustomDeadLayer 1 1 0
/DetSys/det/addGriffinCustomDetector 1
/DetSys/det/SetCustomDeadLayer 2 2 0
/DetSys/det/addGriffinCustomDetector 2
/DetSys/det/SetCustomDeadLayer 3 3 0
/DetSys/det/addGriffinCustomDetector 3
/DetSys/det/SetCustomDeadLayer 4 4 0
/DetSys/det/addGriffinCustomDetector 4
/DetSys/det/SetCustomDeadLayer 5 5 0
/DetSys/det/addGriffinCustomDetector 5
/DetSys/det/SetCustomDeadLayer 6 6 0
/DetSys/det/addGriffinCustomDetector 6
/DetSys/det/SetCustomDeadLayer 7 7 0
/DetSys/det/addGriffinCustomDetector 7
/DetSys/det/SetCustomDeadLayer 8 8 0
/DetSys/det/addGriffinCustomDetector 8
/DetSys/det/SetCustomDeadLayer 9 9 0
```

```
/DetSys/det/addGriffinCustomDetector 9
/DetSys/det/SetCustomDeadLayer 10 10 0
/DetSys/det/addGriffinCustomDetector 10
/DetSys/det/SetCustomDeadLayer 11 11 0
/DetSys/det/addGriffinCustomDetector 11
/DetSys/det/SetCustomDeadLayer 12 12 0
/DetSys/det/addGriffinCustomDetector 12
/DetSys/det/SetCustomDeadLayer 13 13 0
/DetSys/det/addGriffinCustomDetector 13
/DetSys/det/SetCustomDeadLayer 14 14 0
/DetSys/det/addGriffinCustomDetector 14
/DetSys/det/SetCustomDeadLayer 15 15 0
/DetSys/det/addGriffinCustomDetector 15
/DetSys/det/SetCustomDeadLayer 16 16 0
/DetSys/det/addGriffinCustomDetector 16

/control/verbose 1
/run/verbose 1
/event/verbose 0
/tracking/verbose 0

/DetSys/phys/SelectPhysics emlivermore
/run/initialize
/process/em/fluo true
/process/em/auger true
/process/em/pixe true

#/control/execute vis.mac

###################### USER DEFINED RAD DECAY FILES ##############
/grdm/setRadioactiveDecayFile 27 60 UserData/UserRadData_z27.a60
/grdm/setPhotoEvaporationFile 28 60 UserData/UserEvapData_z28.a60

# Angular Correlations
/grdm/setMultipoleFile 28 60 UserData/UserMultipoleData_z28.a60
```

```
/grdm/setMultipoleGroundStateSpinAngularMomentum 28 60 0.0
#####################################################################

/gun/particle ion
/gun/ion 27 60
/grdm/nucleusLimits 60 60 27 27

/run/beamOn 10000000
```

Appendix B

Simulation Multipolarity File

```
// This is the UserMultipoleData_z28.a60 file

// Energy level, gamma-ray energy, E, M, Mixing
1.332518e+03 1.332501e+03   2 0 0
2.505766e+03 1.173237e+03   2 0 0
```

Appendix C

Experimental Angular Correlations Algorithm

```
//g++ experimentalcobalt.cpp -I$GRSISYS/include -L$GRSISYS/libraries
    -lGriffin -lTigress -lGRSIDetector -lGRSIFormat -lSceptar `root-config
    --cflags --glibs` -lPhysics -o experimentalcobalt

// This code is specifically written for experimental Co-60 data using
    single crystal positions (no addback)

// C++ headers:
#include <cstdio>
#include <iostream>
#include <fstream>
#include <TMath.h>
#include <sstream>
#include <string>

// ROOT headers:
#include "TFile.h"
#include "TTree.h"
#include "TH1.h"
#include "TCanvas.h"
#include "TVector3.h"
```

```
#include "TApplication.h"
#include "TTreeIndex.h"
#include "TVirtualIndex.h"

// User headers:
#include "TGriffin.h"

using namespace std;

int experimentalcobalt (TTree *AnalysisTree = 0,const char *nuc="")
{

  if(AnalysisTree==0)
    return 1;

  TGriffin *tgrif = 0;
  TGriffinHit *tgrif_hit1 = 0;
  TGriffinHit *tgrif_hit2 = 0;

  TH1F* coinchist = new TH1F("coinchist","Histogram of Coincident
      Gamma-Rays",180,0,180);
  TH1F* norm1 = new TH1F("norm1","Angular Distribution of
      Gamma-Rays",180,0,180);
  TH1F* coshist = new TH1F("coshist","Cosine of the Angular
      Distribution",1000,-1,1);
  TH1F* cossqhist = new TH1F("cossqhist","Cosine Squared of the Angular
      Distribution",1000,0,1);

  string ray1 = " ";
  string ray2 = " ";

  int ray1val, ray2val;
  int numentries = AnalysisTree->GetEntries();

  AnalysisTree->SetBranchAddress("TGriffin", &tgrif);
```

```
printf("\n");
printf("\tHello! Welcome to the gamma-gamma angular correlations code
    :)\t\n");
printf("\n");
printf("\tThis code analyses experimental Cobalt-60 data");
printf("\n");
printf("\tGamma-ray1 set to: 1173.0 keV\n");
printf("\tGamma-ray2 set to: 1332.0 keV\n");
ray1val = 1173.0;
ray2val = 1332.0;
printf("\n");

for (int i = 0; i < numentries; i++) {
  AnalysisTree->GetEntry(i);
  int mult = tgrif->GetMultiplicity();

  if(i%5000 == 0) { printf("\tI am currently processing entry: %i / %i
      \r",i,numentries); }
  if (mult > 2) continue;

  for (int j = 0; j < mult; j++) {
    tgrif_hit1 = tgrif->GetGriffinHit(j);
    Double_t energy1 = tgrif_hit1->GetEnergyLow();

    if((fabs(energy1-ray1val) > 5) && (fabs(energy1-ray2val) > 5))
       continue;

    for (int k = j + 1; k < mult; k++) {
      tgrif_hit2 = tgrif->GetGriffinHit(k);
      Double_t energy2 = tgrif_hit2->GetEnergyLow();

      if((fabs(energy2-ray1val) > 5) && (fabs(energy2-ray2val) > 5))
         continue;
```

```
      TVector3 vect1 = tgrif_hit1->GetPosition();
      TVector3 vect2 = tgrif_hit2->GetPosition();
      Double_t thetarad = vect1.Angle(vect2);
      Double_t thetadeg = (thetarad)*TMath::RadToDeg();
      Double_t costheta = cos(thetarad);

      coinchist->Fill(thetadeg);
    }
  }
}

printf("\n");
TApplication *app = new TApplication("app",0,0);

map<int,int> griffin_weights;
ifstream infile;
infile.open("normalisations.dat");

if(infile.fail()) {
  cout << "\tCan't open normalisation file - no normalisations for you!"
      << endl;
  return 1;
}

string line;

while (getline(infile,line)) {
  stringstream ss(line);
  int val1, val2;
  ss >> val1; ss >> val2;
  griffin_weights.insert(make_pair(val1,val2));
}

int nonzerobins=0;
```

```
  for(int x=0; x < coinchist->GetNbinsX() ;x++) {
    double val = (double)coinchist->GetBinContent(x);
    if(val<1)
      continue;
    nonzerobins++;
    double weight = 1.0;
    if(griffin_weights.count(x)) {
      weight = (double)griffin_weights.at(x);
    }
    norm1->SetBinContent(x,val/weight);
    norm1->SetBinError(x,sqrt(val)/weight);
  }

  for(int x=0; x < norm1->GetNbinsX() ;x++) {
    double val = (double)norm1->GetBinContent(x);
    double err = (double)norm1->GetBinError(x);
    double cosang = TMath::Cos(((double)x)*TMath::DegToRad());
    double cossqang = (pow(cosang,2));
    coshist->Fill(cosang,val);
    coshist->SetBinError(coshist->FindBin(cosang),err);
    cossqhist->Fill(cossqang,val);
    cossqhist->SetBinError(cossqhist->FindBin(cossqang),err);
  }

  coshist->SaveAs("ExperimentalHist.C");
  coshist->Draw();

  app->Run(true);
}

#ifndef __CINT__

int main(int argc, char **argv)
{
```

```
  if(argc < 2) {
    printf("\tTry ./codata <analysisxxxxx_xxx.root instead.\n");
    return 1;
  }

  const char *nuc = "";

  if(argc == 3) {
    nuc = argv[2];
  }

  TFile f(argv[1]);
  TTree *tree = (TTree*)f.FindObjectAny("AnalysisTree");

  experimentalcobalt(tree,nuc);

  return 0;
}

#endif
```

Appendix D

Simulation Angular Correlations Algorithm

```
//g++ -g simulatedcobalt.cpp `root-config --cflags --libs` -o
    simulatedcobalt

// I have made this specific to my simulated Cobalt-60 data using single
    crystal positions

#include <cstdio>
#include <iostream>
#include <fstream>
#include <vector>
#include <utility>
#include <sstream>
#include <map>
#include <math.h>

#include <TROOT.h>
#include <TLeaf.h>
#include <TMath.h>
#include <TList.h>
#include <TFile.h>
#include <TDirectory.h>
```

```
#include <TTree.h>
#include <TVector3.h>
#include <TH1.h>
#include <TH2.h>

using namespace std;

struct AddbackHit
{

  Double_t energy;
  Double_t maxEnergy;
  Int_t detNumber;
  Int_t cryNumber;

};

TList *InitMyHists();
void FillMyHists(vector<AddbackHit>,TList*);
void WriteMyHists(TList*);
void NormaliseHists(TList*);

Double_t xpos[16][4], ypos[16][4], zpos[16][4];

void simulatedcobalt ()
{

  TFile* cobaltdata = new TFile("g4out.root");
  TVector3 ray1;
  TVector3 ray2;
  TDirectory *dir = (TDirectory*)cobaltdata->Get("ntuple");
  TTree *ntuple = (TTree*)dir->Get("ntuple");
  TList *list = InitMyHists();

  int numentries = ntuple->GetEntries();
```

```
Int_t evtlast = 0, evtcurrent = 1;
Double_t detectornum1 = 0, detectornum2 = 0;
Double_t crystalnum1 = 0, crystalnum2 = 0;

ifstream data;
data.open("CrystalPositions.txt");

if( data.fail() ) {
  cout << "\tError opening CrystalPositions.txt\n" << endl;
  return;
}

Int_t det, cry;
Double_t x, y, z;
Double_t xcoord1, xcoord2, ycoord1, ycoord2, zcoord1, zcoord2;

while (data.good()) {

  string line;
  getline(data, line);
  istringstream iss(line);

  iss >> det;
  iss >> cry;
  iss >> x;
  iss >> y;
  iss >> z;

  xpos[det][cry] = x;
  ypos[det][cry] = y;
  zpos[det][cry] = z;
}

data.close();
```

```
vector<Double_t> vec_edep;
vector<Int_t> vec_detectornumber;
vector<Int_t> vec_crystalnumber;
vector<AddbackHit> cloverHits;

Double_t totalE;
printf("\t\n");

for (int i = 0; i < numentries; i++) {
  ntuple->GetEntry(i);
  Double_t ptype = ntuple->GetLeaf("particleType")->GetValue(0);

  if ( ptype != 1 )
    continue;

  if((i%50000)==0) {
    printf("\t I am on entry: %i / %i    \r",i,numentries);
  }

  Double_t edep = ntuple->GetLeaf("depEnergy")->GetValue(0);
 Int_t detectornum = ntuple->GetLeaf("detNumber")->GetValue(0);
 Int_t crystalnum = ntuple->GetLeaf("cryNumber")->GetValue(0);
 Int_t eventno = ntuple->GetLeaf("eventNumber")->GetValue(0);

  if(evtlast == eventno) {
    vec_edep.push_back(edep);
   vec_detectornumber.push_back(detectornum);
   vec_crystalnumber.push_back(crystalnum);
   continue;
  } else {
    Double_t emax = 0.0;
   Bool_t foundDetector;
   Int_t idx;
    cloverHits.clear();
    totalE = 0.0;
```

```
for(int j=0; j<vec_edep.size(); j++) {
  foundDetector = false;

  for (idx=0; idx < cloverHits.size(); idx++) {
    if (cloverHits.at(idx).detNumber == vec_detectornumber.at(j)) {
    //foundDetector = true;
     //cloverHits[idx].energy += vec_edep.at(j);
     if (cloverHits.at(idx).cryNumber == vec_crystalnumber.at(j)) {
        foundDetector = true;
        cloverHits[idx].energy += vec_edep.at(j);
      }

      if (vec_edep.at(j) > cloverHits[idx].maxEnergy) {
        cloverHits[idx].maxEnergy = vec_edep.at(j);
       cloverHits[idx].cryNumber = vec_crystalnumber.at(j);
      }
    }
  }

  if (!foundDetector) {
    AddbackHit hit;
    hit.energy = vec_edep.at(j);
    hit.maxEnergy = vec_edep.at(j);
    hit.cryNumber = vec_crystalnumber.at(j);
    hit.detNumber = vec_detectornumber.at(j);

    cloverHits.push_back(hit);
  }
}
vec_edep.clear();
vec_detectornumber.clear();
vec_crystalnumber.clear();

vec_edep.push_back(edep);
```

```
      vec_detectornumber.push_back(detectornum);
      vec_crystalnumber.push_back(crystalnum);
     evtlast = eventno;

      FillMyHists(cloverHits,list);
   }
  }
  NormaliseHists(list);
  WriteMyHists(list);
}

TList *InitMyHists() {

  TList *list = new TList();

  list->Add(new TH2F("energy_cry","energy_cry",100,0,100,4000,0,4000));
  list->Add(new
      TH2F("energy_angle_1173","energy_angle_1173",180,0,180,4000,0,4000));
  list->Add(new
      TH2F("energy_angle_1332","energy_angle_1332",180,0,180,4000,0,4000));

  list->Add(new TH1F("counts_angle","counts_angle",180,0,180));
  list->Add(new TH1F("counts_cosang","counts_cosang",1000,-1,1));
  list->Add(new TH1F("counts_cos2ang","counts_cos2ang",1000,0,1));

  list->Add(new TH1F("counts_angle_norm","counts_angle_norm",180,0,180));
  list->Add(new TH1F("counts_cosang_norm","counts_cosang_norm",1000,-1,1));
  list->Add(new TH1F("counts_cos2ang_norm","counts_cos2ang_norm",1000,0,1));

  printf("\n\t Histograms have been initialised... \t\n");

  return list;
}

void FillMyHists(vector<AddbackHit> hits,TList *list) {
```

```
TH2F *h2 = 0;
TH1F *h1 = 0;
TVector3 vec_x;
TVector3 vec_y;

for(int x=0;x<hits.size();x++) {
  Double_t arraynumber = (hits[x].detNumber*4)+hits[x].cryNumber+1;
  h2 = (TH2F*)list->FindObject("energy_cry");

  if(h2) h2->Fill(arraynumber,hits[x].energy);

  for(int y=x+1;y<hits.size();y++) {
    vec_x.SetXYZ(xpos[hits[x].detNumber][hits[x].cryNumber],
                 ypos[hits[x].detNumber][hits[x].cryNumber],
                 zpos[hits[x].detNumber][hits[x].cryNumber]);
    vec_y.SetXYZ(xpos[hits[y].detNumber][hits[y].cryNumber],
                 ypos[hits[y].detNumber][hits[y].cryNumber],
                 zpos[hits[y].detNumber][hits[y].cryNumber]);
    if(fabs(hits[x].energy - 1173.0) < 5) {
      h2 = (TH2F*)list->FindObject("energy_angle_1173");
      double theta = vec_x.Angle(vec_y);
      if(h2) h2->Fill(theta*TMath::RadToDeg(),arraynumber,hits[y].energy);
    }

    if(fabs(hits[x].energy - 1332.0) < 5) {
      h2 = (TH2F*)list->FindObject("energy_angle_1332");
      double theta = vec_x.Angle(vec_y);
      if(h2) h2->Fill(theta*TMath::RadToDeg(),arraynumber,hits[y].energy);
    }

    if(((fabs(hits[x].energy - 1173.0) < 5) && (fabs(hits[y].energy -
        1332.0) < 5)) ||
       ((fabs(hits[y].energy - 1173.0) < 5) && (fabs(hits[x].energy -
          1332.0) < 5))) {
```

```
        double theta = vec_x.Angle(vec_y);
        h1 = (TH1F*)list->FindObject("counts_angle");
        if(h1)h1->Fill(theta*TMath::RadToDeg());
        h1 = (TH1F*)list->FindObject("counts_cosang");
        double costheta = TMath::Cos(theta);
        double cossqtheta = pow(costheta,2);
        if(h1)h1->Fill(costheta);
        h1 = (TH1F*)list->FindObject("counts_cos2ang");
        if(h1)h1->Fill(cossqtheta);
      }
    }
  }
}

void NormaliseHists(TList *list) {

  map<int,int> griffin_weights;
  TH1F *h1=0;
  TH1F *n1=0;
  TH1F *n2=0;
  ifstream infile;
  infile.open("normalisations.dat");

  if(infile.fail()) {
    printf("\tNo normalisations for you :(");
    return;
  }

  string line;
  while ( getline(infile,line)) {
    stringstream ss(line);
    int val1,val2;
    ss >> val1; ss >> val2;
    griffin_weights.insert(make_pair(val1,val2));
```

```
  }

  h1 = (TH1F*)list->FindObject("counts_angle");
  n1 = (TH1F*)list->FindObject("counts_angle_norm");
  printf("\n\n");

  for(int x=1;x<=h1->GetNbinsX();x++) {
    double val = (double)h1->GetBinContent(x);
    if(val<1)
      continue;
    double weight = 1.0;
    if(griffin_weights.count(x)) {
      weight = (double)griffin_weights.at(x);
    }
    n1->SetBinContent(x,val/weight);
    n1->SetBinError(x,sqrt(val)/weight);
  }

  h1 = (TH1F*)list->FindObject("counts_angle_norm");
  n1 = (TH1F*)list->FindObject("counts_cosang_norm");
  n2 = (TH1F*)list->FindObject("counts_cos2ang_norm");

  for(int x=1;x<=h1->GetNbinsX();x++) {
    double val = (double)h1->GetBinContent(x);
    double err = h1->GetBinError(x);
    double cosang = TMath::Cos(((double)x)*TMath::DegToRad());
    n1->Fill(cosang,val);
    n1->SetBinError(n1->FindBin(cosang),err);
    n2->Fill(pow(cosang,2),val);
    n2->SetBinError(n2->FindBin(pow(cosang,2)),err);
  }
  printf("\n\t Histograms have been normalised! \t\n");
}

void WriteMyHists(TList *list) {
```

```
  TFile file("MyHists.root","recreate");
  list->Write();
  file.Close();
  printf("\n\t Histograms have been written to the file 'MyHists.root' :)
      \t\n");
}

#ifndef __CINT__

int main(int argc, char **argv) {

  simulatedcobalt();
  return 0;
};

#endif
```

Appendix E

Legendre Polynomial Fitting Algorithm

```
nkTF1 *MakeLegendre(const char *name, double N, double a2, double a4)
{
  TF1 *f = new TF1(name, "[0]*(1 + [1]*ROOT::Math::legendre(2,x) +
      [2]*ROOT::Math::legendre(4,x))", -1, 1);
  f->SetParameters(N,a2,a4);

  return f;
}

void DrawLegendre(double N, double a2, double a4, Option_t* opt="")
{
  MakeLegendre("leg",N,a2,a4)->Draw(opt);
}

void DoIt(const char *histname, double a2, double a4)
{
  TH1F *hist = (TH1F*)gROOT->FindObject(histname);

  double N = hist->GetMaximum();
  TF1 *f1 = MakeLegendre(Form("%s_fit",histname),N,a2,a4);
  TF1 *f2 = MakeLegendre(Form("%s_th",histname),N,0,0);
```

```
  f2->FixParameter(1,a2);
  f2->FixParameter(2,a4);
  f2->SetLineColor(kBlue);

  hist->Fit(f1);
  hist->Fit(f2,"+");
}

void simulatedlegendre(void)
{
  gSystem->Load("libMathMore.so");

  DoIt("counts_cosang_norm",0.1020,0.0091); // theoretical a2,a4 values for
      4->2->0
}
```

Bibliography

[1] TRIUMF, November 2014. Available at: http://www.triumf.ca/sites/default/files/images/tank4M.jpg.

[2] TRIUMF. GRIFFIN, November 2014. Available at: http://www.triumf.ca/griffin.

[3] The University of Guelph. Descant, November 2014. Avaliable at: http://www.physics.uoguelph.ca/Nucweb/descant.html.

[4] Glenn F. Knoll. *Radiation Detection and Measurement*, pages 398–401. John Wiley and Sons, Inc., 2nd edition, 1989.

[5] K. Ferlic. The phenomenon of pair production, 2006. Avaliable at: http://ryuc.info/creativityphysics/energy/pair_production.htm.

[6] H Paul. File:co60 spectrum.jpg, December 2006. Available at: http://commons.wikimedia.org/wiki/File:Co60_Spectrum.JPG#file.

[7] University of Guelph Department of Physics. News, September 2014. Avaliable at: http://www.physics.uoguelph.ca/Nucweb/.

[8] Tubas-en, November 2014. Available at: http://commons.wikimedia.org/wiki/File:Cobalt-60m-decay.svg.

[9] Evan Rand. Geant4 Gamma-Gamma Angular Correlations. Technical report, University of Guelph, August 2014.

[10] The University of Guelph. Griffin, November 2014. Available at: http://www.physics.uoguelph.ca/Nucweb/griffin.html.

[11] TRIUMF. HPGe Coordinate Table, November 2014. Available at: http://www.triumf.info/wiki/tigwiki/index.php/HPGe_Coordinate_Table.

[12] TRIUMF. About TRIUMF: History, November 2014. Available at: http://www.triumf.ca/home/about-triumf/history.

[13] TRIUMF. Research Topics, November 2014. Available at: http://www.triumf.ca/research-program/research-topics.

[14] Guinness World Records. Largest Cyclotron, November 2014. Available at: http://www.guinnessworldrecords.com/world-records/largest-cyclotron/.

[15] Nicholas Leach. Science Ambassador Program, 2014. Version 16.

[16] Y.-N. Rao R. Baartman. Investigation of space charge effect in TRIUMF injection beamline. Research Note, TRIUMF, 2003.

[17] Dr. David Stout. Cyclotrons and Radiochemistry. Available at: http://www.crump.ucla.edu/start/course/Lecture%202%20-%20Cyclotrons%20Explained%201-3.pdf, 2012.

[18] TRIUMF. A few "quick facts" about the TRIUMF cyclotron, November 2014. Available at: https://cycops.triumf.ca/cycfac.htm.

[19] TRIUMF. Main Cyclotron and Beam Lines, November 2014. Available at: http://www.triumf.ca/research-program/research-facilities/main-cyclotron-beam-lines.

[20] Dominik Krauss. Production of radioactive ion beams via the ISOL technique. Available at: http://www.mpa-garching.mpg.de/lectures/ADSEM/SS13_Krauss.pdf, June 2012.

[21] TRIUMF. ISAC Facilities for Rare-Isotope Beams, November 2014. Available at: http://www.triumf.ca/research/research-facilities/isac-facilities-for-rare-isotope-beams.

[22] P. E. Garrett A. B. Garnsworthy. The 8pi spectrometer. *Hyperfine Interact*, 225:121–125, 2014.

[23] Oak Ridge National Laboratory. Low-energy Radioactive Ion Beam Decay Spectroscopy Station at HRIBF. Research Note, Oak Ridge National Laboratory, 2007.

[24] Inc. CANBERRA Industries. High-purity Germanium (HPGe) Detectors, November 2014. Availiable at: http://www.canberra.com/products/detectors/germanium-detectors.asp?Accordion1=0.

[25] A. B. Garnsworthy C. E. Svensson. The GRIFFIN Spectrometer. *Hyperfine Interact*, 225:127–1132, 2014.

[26] ORTEC. Nuclear Applications Software, November 2014. Avaliable at: http://www.ortec-online.com/Solutions/applications-software.aspx.

[27] Kenneth S. Krane. *Introductory Nuclear Physics*, page 160. John Wiley and Sons, Inc., Wiley-India edition, 1988.

[28] Advanced Physics Laboratory. Gamma Ray Spectroscopy. Technical report, University of Florida, 2014. Available at: http://www.phys.ufl.edu/courses/phy4803L/group_I/gamma_spec/gamspec.pdf.

[29] Melanie A. Pelcher Theodore A. Rapach. Gamma Ray Spectroscopy. Technical report, University of Rochester, 2014. Availabe at: http://www.pas.rochester.edu/~advlab/reports/pelcher_rapach_gammaspec.pdf.

[30] S. E. Rowan W. J. O'Brien. A Gamma-Ray Coincidence Experiment Using Cobalt-60. Available at: http://www.willob.freeserve.co.uk/co60.pdf, April 1998.

[31] The Editors of Encyclopaedia Britannica. Parity, January 2015. Availabe at: http://www.britannica.com/EBchecked/topic/443987/parity.

[32] Curran D. Muhlberger. Experiment IX: Angular Correlation of Gamma Rays. Technical report, University of Maryland, May 2008. Availabe at: http://pages.physics.cornell.edu/~cmuhlberger/documents/phys405-paper.pdf.

[33] C. F. Coleman. The Analysis of Angular and Direction-Polarisation Correlation Measurements on Mixed Transitions. *Nuclear Physics*, 5:495–503, 1958.

[34] Peter C. Bender. *Nuclear Structure of Neutron Rich 34P using In-Beam Gamma Ray Spectroscopy.* PhD thesis, Florida State University, 2011.

[35] T. Yamazaki. Tables of Coefficients for Angular Distribution of Gamma-Rays from Aligned Nuclei. *Atomic Data and Nuclear Data Tables*, 13:391–406, 1974.

[36] D. M. Brink H. J. Rose. Angular Distributions of Gamma-Rays in Terms of Phase-Defined Reduced Matrix Elements. *Reviews of Modern Physics*, 39, Number 2:306–347, 1967.

[37] A. W. Sunyar E. Der Mateosian. Tables of Attenuation Coefficients for Angular Distribution of Gamma-Rays from Partially Aligned Nuclei. *Nuclear Data*, 3:1–23, 1967.

[38] H. A. Tolhoek J. A. M. Cox. Gamma Radiation Emitted by Oriented Nuclei. *Physica*, XIX:673–682, 1953.

[39] Geant Collaboration. Geant4 Status and Results. Technical report, Geant4 Collaboration, 2000. Available at: `http://geant4.cern.ch/results/papers/chep2000-a140.pdf`.

[40] Geant4 Collaboration. *Geant4 User's Guide for Application Developers*, geant4 10.1 edition, December 2014.

[41] CERN. ROOT User's Guide. Technical report, CERN, 2013. Available at: `https://root.cern.ch/root/html534/guides/users-guide/ROOTUsersGuideA4.pdf`.

[42] TRIUMF. The TRIUMF TIGRESS Facility, August 2003. Avaliable at: `http://www.triumf.ca/headlines/current-events/triumf-tigress-facility`.

[43] Adam Garnsworthy. First Experiments Performed With GRIFFIN, December 2014. Avaliable at: `http://www.triumf.ca/headlines/current-events/first-experiments-performed-griffin`.